TRANSCRIPTOMIC SIGNATURES OF TELOMERASE-DEPENDENT AND -INDEPENDENT AGEING, IN THE ZEBRAFISH GUT AND BRAIN

Raquel Martins, Michael Rera, Catarina Henriques

TRANSCRIPTOMIC SIGNATURES OF TELOMERASE-DEPENDENT AND -INDEPENDENT AGEING, IN THE ZEBRAFISH GUT AND BRAIN

Running title: Kinetics of ageing in the zebrafish gut and brain

AUTHORS

Raquel R. Martins[1], Michael Rera[2] and Catarina M. Henriques[1]

Affiliations :

1. The Bateson Centre, Healthy Lifespan Institute and Department of Oncology and Metabolism, University of Sheffield Medical School, Sheffield, UK.

2. Université de Paris / Inserm- Centre de Recherche Interdisciplinaire (CRI Paris)

Corresponding author: c.m.henriques@sheffield.ac.uk

SUMMARY

Telomerase is best known for its role in the maintenance of telomere length and its implications for ageing and cancer. The mechanisms, kinetics and tissue-specificity underlying the protective or deleterious mechanisms of telomerase, however, remain largely unknown. Here, we sought to determine the telomerase-dependent and -independent transcriptomic changes with ageing, in the gut and brain, as examples of high and low proliferative tissues, respectively. We hypothesised this could shed light on common telomerase-dependent and -independent therapeutic targets aimed at preventing or ameliorating age-associated dysfunction in both tissues. For this, we used the zebrafish model which, similarly to humans, depends on telomerase for health- and lifespan. We performed whole tissue RNA sequencing of gut and brain, in naturally aged zebrafish alongside prematurely aged telomerase null mutants (*tert*$^{-/-}$), throughout their lifespan. Our study highlights stem cell exhaustion as the first main hallmark of ageing to be de-regulated in WT zebrafish gut and brain. Towards the end of life, altered intercellular communication becomes the main hallmark of ageing de-regulated in both gut and brain, and this is accelerated in both tissues, in the absence of telomerase. Finally, we identify 7 key gene changes common between the gut and brain at the early stages of ageing, highlighting

potential early intervention therapeutic targets for preventing age-associated dysfunction in both tissues.

KEYWORDS: Ageing, telomerase, telomeres, gut, brain, zebrafish, transcriptomics, RNA sequencing

1 INTRODUCTION

Ageing is the strongest risk factor for chronic diseases. How and why this is the case remain important questions in the field, especially as key research has shown that targeting common hallmarks of ageing, such as cellular senescence (Baker et al., 2016; Baker et al., 2011), can have a positive impact across multiple tissues and ameliorate several chronic diseases of ageing at the same time. There are well-known key hallmarks of ageing, such as genomic instability, telomere attrition, epigenetic alterations, loss of proteostasis, de-regulated nutrient sensing, mitochondrial dysfunction, cellular senescence, stem cell exhaustion and altered intercellular communication(Lemoine, 2021; López-Otín, Blasco, Partridge, Serrano, & Kroemer, 2013) . However, a major challenge in ageing research is to identify where and when these potentially pathological changes start and when the tipping point between homeostasis and loss of function takes place (Rando & Wyss-Coray, 2021). Additionally, several lines of evidence suggest there may be specific tissues where age-related changes start earlier, potentially influencing others (de Jong, Gonzalez-Navajas, & Jansen, 2016; Rera, Azizi, & Walker, 2013). One example is the gut, which has been suggested to be a trigger for multiple organ failure (Cardoso et al., 2008). Evidence suggests that the kinetics of ageing can vary dramatically between cells, tissues (Shokhirev & Johnson, 2021; M. J. Zhang, Pisco, Darmanis, & Zou, 2021) and individuals, and that this is influenced not only by intrinsic but also extrinsic factors, recently discussed elsewhere (Rando & Wyss-Coray, 2021). These considerations are of particular importance when the aim is to understand how changes in ageing lead to disease and how, when and where to intervene. This is crucial in order to shift towards a more preventive form of medicine, which is a current global ambition (Rudnicka et al., 2020), aiming to match the dramatic increase of lifespan we have experienced in the past century, with an equivalent increase in years of healthy living, i.e, healthspan (England, 2017).

Tissue-specific transcriptomics analysis over the lifecourse can offer important insights into the downstream molecular mechanisms potentially driving the pathology of ageing.

Significant research is being dedicated to these approaches in different animal models, including in mice (Schaum et al., 2020; Tabula Muris, 2020; M. J. Zhang et al., 2021). Different animal models may offer different insights into the mechanisms of ageing, and some models may be better suited to explore the role of specific human hallmarks of ageing. The role of telomere attrition in natural ageing can be considered a hallmark of ageing that may benefit from additional and complementary models, beyond the mouse (Forsyth, Wright, & Shay, 2002; Gomes et al., 2011; Sullivan et al., 2021). Once such model is the zebrafish that, like humans, age and die in a telomerase-dependent manner (Anchelin et al., 2013; Carneiro, de Castro, & Ferreira, 2016; Madalena C Carneiro et al., 2016; Henriques, Carneiro, Tenente, Jacinto, & Ferreira, 2013; Henriques & Ferreira, 2012). Restricted telomerase expression and function are key determinants of natural ageing in humans, underpinning multiple age-related diseases (Blackburn, Epel, & Lin, 2015). However, the role and the dynamics of telomerase-dependent changes that may contribute to tissue-specific ageing are still poorly understood. This is partially due to the fact that telomerase appears to have multiple functions in the cell, that go beyond the maintenance of telomere length, recently reviewed elsewhere (Segal-Bendirdjian & Geli, 2019).

Telomerase is best known for its telomere-dependent function (i.e. canonical functions), acting as a reverse transcriptase, maintaining telomere length through its catalytic domain (TERT protein) and RNA template (TERC) (Greider & Blackburn, 1985). Telomeres are $(TTAGGG)_n$ DNA repeats that together with a complex of proteins (known as Shelterin) create a “cap-like” structure at the end of linear chromosomes (de Lange, 2004), preventing the ends of linear chromosomes from being recognised as deleterious DNA double strand breaks (Ferreira, Miller, & Cooper, 2004). However, in humans, due to time- and cell-specific-limited telomerase expression, telomeres shorten with ageing, leading to proliferative exhaustion and replicative senescence (Bodnar, 1998; d'Adda di Fagagna et al., 2003). Importantly, there is accumulation of cellular senescence with ageing in humans (Dimri et al., 1995) and senescence has been linked to several age-associated diseases (Ovadya & Krizhanovsky, 2014). Additionally, short telomeres themselves can lead to de-regulated gene expression, particularly in genes near the chromosome ends, due to loss of the “telomere positioning effect” (TPE), which is known to regulate gene expression of genes at least up to 10MB away from the chromosome ends (Robin et al., 2014).

Growing evidence now suggests that telomerase also has activity independent of its action at telomeres, known as non-canonical (Goodman & Jain, 2011; Romaniuk et al., 2018; Segal-Bendirdjian & Geli, 2019; Sung, Ali, & Lee, 2014). In the nucleus, these non-canonical functions include transcriptional regulation of genes involved in inflammation, including nuclear factor kappa B (NFkB) and tumour necrosis factor alpha (TNFα) (Deacon & Knox, 2018; Ghosh et al., 2012; Mattiussi, Tilman, Lenglez, & Decottignies, 2012), as well as genes involved in cell proliferation (Choi et al., 2008; Sarin et al., 2005) and cell survival (Cao, Li, Deb, & Liu, 2002; Rahman, Latonen, & Wiman, 2005). Telomerase can also translocate to the mitochondria, where it has been shown to play a protective role against DNA damage and oxidative stress (Ahmed et al., 2008; Haendeler et al., 2009).

As tissues with high cellular turnover present accelerated telomere erosion (Bodnar, 1998; H. W. Lee et al., 1998), it is reasonable to think that telomerase functions are likely to primarily affect highly proliferative tissues. Accordingly, premature accumulation of critically short telomeres has been identified in high proliferative tissues such as the gut, in tert-deficient animal models. Nonetheless, the role of telomerase and telomeres is not restricted to highly proliferative tissues. In the brain, considered a predominately post-mitotic tissue, telomerase has been shown to have a protective role against excitotoxicity (Eitan et al., 2012), oxidative stress (Spilsbury, Miwa, Attems, & Saretzki, 2015), and neuronal death (J. Lee et al., 2010), all involved in neurodegenerative diseases. Studies in late-generation telomerase-deficient mice have suggested that limited telomerase expression is associated with premature accumulation of senescence-associated markers in different cell populations including Purkinje neurons, cortical neurons and microglia (De Felice et al., 2014; Jaskelioff et al., 2011; Jurk et al., 2012; Raj et al., 2015). Telomerase is therefore a promising target to promote healthy ageing in multiple tissues and so the identification of mechanisms driving telomerase-dependent ageing could enable the identification of targeted therapies to improve healthspan.

In this study, we aimed to determine the telomerase-dependent and -independent transcriptomic changes and their kinetics occurring during ageing, in both brain and gut within the same individuals. We hypothesised that this would allow us to identify key age-associated genes and pathways that become prematurely de-regulated in both or either tissue, providing key insights into the early stages of ageing in these tissues and likely

interactions. We further hypothesised that this may highlight potential common telomerase-dependent and -independent therapeutic targets for early intervention aimed at preventing age-associated dysfunction in both tissues. To address these questions, we performed RNA sequencing in whole tissues (gut and brain) of WT fish (2, 9, 22 and 35 months of age) alongside telomerase mutant fish (*tert*$^{-/-}$) (2, 9 and 22 months of age). *tert*$^{-/-}$ zebrafish, extensively characterised elsewhere (Anchelin et al., 2013; Madalena C Carneiro et al., 2016; Henriques et al., 2013), display no telomerase activity and have significantly shorter telomeres from birth, consequently ageing and dying prematurely. Ageing is usually described as a time-dependent change in tissue homeostasis, that increases the probability of disease and death (Hayflick, 2007). However, whether the genes and pathways driving or accompanying these time-dependent changes are also consistently changing in a time-specific manner, remains unresolved (Rando & Wyss-Coray, 2021). We therefore decided to combine a time-series analysis (STEM), which allowed the identification of genes and pathways that are consistently up or down-regulated over-time, with the more traditional differential gene expression (DEGs) analysis between young and old animals. This combined strategy allowed the identification of genes that change in a monotonic, time-dependent manner (STEM), versus genes that change at specific stages of life (DEGs).

We show that although the gut and brain have distinct transcriptomic signatures of ageing, both tissues display hallmarks of ageing as early as 9 months in the WT zebrafish. Importantly, telomerase depletion accelerates the appearance of such hallmarks in both gut and brain. In particular, we identify stem cell exhaustion as the common principal hallmark of ageing at the early stages of ageing, in both tissues. Further, we identify altered intercellular communication, in which immunity and inflammation play a central role, as the main telomerase-dependent hallmark of ageing common between the gut and brain. Finally, we conclude that the gut displays telomerase-dependent hallmarks of ageing at an earlier age than the brain and that these include changes in several key genes that have also been included in the GenAge database, a benchmark curated database that included genes involved in ageing across different organisms, including in humans (Tacutu et al., 2018). Finally, we identify 7 key gene changes common between the gut and brain at the early stages of ageing, namely *ccnb1, kif2c, serpinh1a, temem37*, *si:ch211-5k11.8*, *cfap45* and *eif4ebp3l*.

2 RESULTS

2.1 Identification of monotonic, time-dependent gene signatures and process changes with ageing in the zebrafish gut and brain

In order to identify telomerase-dependent and -independent transcriptional signatures of ageing in the zebrafish gut and brain, we performed RNA-Sequencing of whole tissues, throughout the lifespan of WT and telomerase-deficient (*tert*$^{-/-}$) fish (**Fig. 1 and source data**). While *tert*$^{-/-}$ fish have a lifespan of c. 12-20 months, WT fish typically die between c. 36-42 months of age (Madalena C Carneiro et al., 2016). The data shown here include 4 age-groups of WT (2, 9, 22 and >30 months), corresponding to young, adult, median lifespan and old. As the *tert*$^{-/-}$ fish have a shorter lifespan compared with their WT siblings, the data include 3 age-groups of telomerase-deficient fish (2, 9, and 22 months), which correspond to young, medium lifespan and old. Each group has a sample size of 3 animals and the brains and guts from within the same groups of animals were used (**Fig 1A**). The reads were aligned to the latest zebrafish genome build GRCz11 (Lawson et al., 2020) and resulted in uniquely mapped read percentages ranging from 92.1% to 94.4%, which is a readout of good quality (Lawson et al., 2020). All samples had at least 10 million uniquely mapped reads, except G11 which had around 8 million. Further quality control, using a principal component analysis (PCA) including all the samples, revealed that one of the gut samples clustered with the brain samples, and not with the gut samples (**Fig. 1B**). This was considered to be a technical error and this sample (G7) was therefore excluded from further analysis. To analyse the overall impact of the genotype and age on transcriptomic regulation, we then performed a PCA in the samples from the gut and brain, separately. We further observed that some samples cluster *per* age, but there are some genotypes that separate quite distinctly, despite being of the same age (**Fig 1C and D**). As an example, the WT and *tert*$^{-/-}$ gut samples are quite distinct, and the *tert*$^{-/-}$ 2-month samples cluster closely to the WT at 9 months than the WT at 2 months (**Fig 1C**), providing the first hint of an acceleration of the ageing transcriptomic profile in the *tert*$^{-}$/-. We found that there was higher variability in the gut than in the brain, between samples within each age group (**Fig 1C and D**). A summary of the number of significant differentially expressed genes (DEGs) in all samples is represented in **Fig. 1E**. How these DEGs relate to which other, how many

186 overlap and how many are in common or accelerated in the absence of telomerase (*tert*$^{-/-}$),
187 will be explored later in the manuscript.

188 To identify genes and pathways that are consistently up- or down-regulated in a time-
189 dependent manner in natural ageing in the zebrafish gut and brain, we grouped the genes
190 into temporal expression profiles, by time-series analysis using Short Time-series Expression
191 Miner (STEM) software (Ernst & Bar-Joseph, 2006). To determine whether the temporal
192 profiles were associated with specific biological processes and pathways, pathway over-
193 representation analysis (ORA) were performed for the genes assigned to the significant
194 STEM profiles. Enrichments of GO Biological Process (GOBP), GO Molecular Function
195 (GOMF), GO Cellular Compartment (GOCC), Kyoto Encyclopedia of Genes and Genomes
196 (KEGG) terms and REACTOME pathway terms were therefore analysed for each profile.
197 Time-series analysis of WT gut identified 9 different profiles, with 2 of them containing up-
198 regulated genes (profiles 7 and 21. Total of 523 genes), and 7 containing down-regulated
199 genes (profiles 32, 31, 23, 9, 12, 22 and 34. Total of 11,594 genes) (**Fig. 2A1 and source**
200 **data**). Interestingly, in the *tert*$^{-/-}$ gut, all the profiles identified by time-series analysis contain
201 up-regulated genes (profiles 8, 6, 15 13, 12 and 11. Total of 10,317 genes) (**Fig. 2A2 and**
202 **source data**). Enrichment analysis showed that the profiles containing up-regulated genes
203 are associated with immune response, while profiles containing down-regulated genes are
204 largely associated with proliferation, cellular response to DNA damage, and DNA damage
205 repair, in both WT and *tert*$^{-/-}$ gut (**Fig. 2 A1.1, 1.2 and A2.1**). To help contextualise our
206 analysis, we performed a further classification of enriched processes according to the
207 hallmarks of ageing, which have been previously identified (Lemoine, 2021; López-Otín et
208 al., 2013). This classification further strengthened the observation that the up-regulated
209 profiles include genes mostly involved in altered intercellular communication, in which
210 immunity and inflammation play a key role, whereas the down-regulated profiles identify
211 stem cell exhaustion and genomic instability as the main hallmarks of ageing, to which the
212 genes affecting proliferation, DNA damage and repair are likely to contribute (**Fig. 2 A1.1,**
213 **1.2 and A2.1 and source data)**.

214 In the WT brain, we identified 9 temporal profiles, 6 of them including up-regulated
215 genes (profiles 42, 29, 40, 30, 21 and 48. Total of 7,230 genes), and 3 including down-
216 regulated genes (profiles 1, 12 and 26. Total of 561 genes) (**Fig. 2B1 and source data**). In the

217 *tert*$^{-/-}$ brain, time-series analysis revealed 6 different profiles. Profiles 4, 0 and 3 containing
218 down-regulated genes (total of 5,374 genes) and profiles 15, 12 and 11 containing up-
219 regulated genes (total of 1,155 genes) (**Fig. 2B2 and source data**). As in the gut, up-
220 regulated profiles reveal genes mostly involved in immune regulation and inflammation and
221 down-regulated profiles are mostly involved in cell cycle, genome stability and DNA damage
222 responses, in both genotypes This is further highlighted when placed into context by the
223 analysis based on the hallmarks of ageing, where up-regulated profiles identify altered
224 intercellular communication whereas the down-regulated ones identify stem cell exhaustion
225 as the main hallmarks affected (**Fig 2 B1.1, 1.2; B2.1, 2.22 and source data**).

226 In summary, STEM analysis and enrichment pathways in both gut and brain ageing
227 show a general trend towards up-regulation of genes involved in immune response and
228 down-regulation of genes involved in cell cycle, DNA damage and repair. This general trend
229 is recapitulated in the absence of telomerase. These mechanisms are all known contributors
230 to the well-described altered intercellular communication, genome stability and stem cell
231 exhaustion hallmarks of ageing, respectively (Lemoine, 2021; López-Otín et al., 2013).

232

233 **2.2 Comparing the hallmarks of ageing over time, in WT and *tert*$^{-/-}$ zebrafish gut and**
234 **brain**

235 More than just identifying the signatures of natural WT ageing in the gut and brain
236 and identifying telomerase-dependent and -independent changes, we wanted to
237 understand if there were particular changes occurring before others, and how their kinetics
238 compared between the gut and the brain. In order to contextualise our analysis in the light
239 of the well-described hallmarks of ageing, (Lemoine, 2021; López-Otín et al., 2013), we used
240 the main hallmarks of ageing as headers in which we could group the different changes in
241 processes that were enriched from both the STEM profiles and all DEGs. This allowed us to
242 compare the effects of age, genotype and tissue on the evolution of the key hallmarks of
243 ageing. When we combine all the gene changes (up- and down-regulated) and associated
244 biological processes affected (**Fig. 3 and source data**), we observe distinct tissue-specific
245 signatures of ageing, namely in the gut (**Fig. 3A**) and brain (**Fig. 3B**), particularly when
246 considering the time-series analysis on its own (STEM) (**Fig 3. A1 and B1**). Whereas ageing in
247 the WT gut seems to be predominantly affected by the de-regulated nutrient sensing

initially, the brain displays stem cell exhaustion as the main hallmark affected at the early age of 9 months (**Fig. 3A1**, **B1**, respectively). When we combine the different analysis, though (**Fig. 3A3 and B3**), both gut and brain have stem cell loss as the main hallmark of ageing associated with the enriched processes found at 9 months of age, highlighting this as a potential contributor to the early stages of ageing in both tissues. Towards the end of life, both gut and brain have altered intercellular communication as the main hallmark of ageing identified. Importantly, independently of the analysis, the *tert*$^{-/-}$ zebrafish show accelerated hallmarks of ageing. In specific, a *tert*$^{-/-}$ 2-month-old gut profile is very similar to a WT 35-month-old gut profile (**Fig. 3A**). In the brain, at 2 months of age the *tert*$^{-/-}$ mutant also displays some of the hallmarks of ageing that also become altered in WT ageing at later ages, particularly altered intercellular communication, but the *tert*$^{-/-}$ brain becomes much more similar to the aged WT from the age of 9 months onwards (**Fig. 3B**). This suggests that hallmarks of ageing accelerated in the absence of telomerase are developing earlier in the gut than in the brain.

Finally, when we look at the overall number of gene expression changes, i.e, not just the ones associated with the hallmarks of ageing, we observe that there is a general increase in the number of changes in gene expression with ageing (**Fig 3 A4 and B4**). However, this increase does not appear to be linear. In specific, in the gut, the number of DEGs is fairly low until 9 months of age, after which there seems to be an inflexion point and the number of DEGs increases up to 5-fold in the oldest WT (>35 months) and 3-fold in the oldest *tert*$^{-/-}$ (22 months). In the brain, there seems to be a more gradual, consistent increase over time, both in WT and *tert*$^{-/-}$. This increase in number of DEGs with ageing may be a consequence of the known de-regulation of gene expression with ageing due to de-repression of heterochromatin and/or changes in epigenetic markers.

2.3 When does a *tert*$^{-/-}$ resemble an aged WT the most?

It is of note that, even though the *tert*$^{-/-}$ accelerates hallmarks of ageing in the gut and brain, the set of genes identified are not necessarily the same as in WT ageing. In specific, looking at the genes at the early stages of ageing, the most significant hallmark of ageing shared between the 2 months old *tert*$^{-/-}$ and WT 9 months gut is nutrient sensing, and only 2 up-regulated genes are in common, namely *lipca (Hepatic triacylglycerol lipase precursor)*

and *pla1a (phospholipase 1a)*. Interestingly, hepatic lipase has been involved in atherogenesis (Santamarina-Fojo, Gonzalez-Navarro, Freeman, Wagner, & Nong, 2004) and age-related macular degeneration diseases that have been hypothesised to have a parallel response to tissue injury induced by multiple factors, including impaired immune responses, and oxidative stress (Neale et al., 2010). In line with the general de-regulated inflammatory response we see in the gut, with ageing (**Figs. 2 and 3 and source data)**, *phospholipase 1a* has been reported to be up-regulated in inflamed gut tissue of Crohn's disease patients (Hong et al., 2017) and has a complex role in the regulation of immunity and inflammation (recently reviewed in (Zhao, Hasse, & Bourgoin, 2021)). In the brain, there are no genes in common between the 2 months old *tert*$^{-/-}$ and WT 9 months associated with altered intercellular communication or genomic instability, the 2 main hallmarks of ageing shared between the genotypes at the early stages of ageing. Following this type of analysis, we could then ask at what age does the *tert*$^{-/-}$ best mimic naturally aged WT, at the level of gene expression. For this, we considered the genes identified within the hallmarks of ageing and the genes classified as "other" i.e. associated with ageing but not obviously associated with the described hallmarks of ageing. We therefore analysed the overlap between all DEGs identified in the old WT (35 months) and the *tert*$^{-/-}$ at the different aged (2, 9 and 22 months), using Venn diagrams created using the Venny 2.1 online platform (Oliveros, 2007-2015) to ask this question. We observe that the 2 months old *tert*$^{-/-}$ has the most genes shared with the 35 months old WT gut (59 genes in common) (**Fig. 4 A1 and Supp. Fig. 1**) whereas it is the *tert*$^{-/-}$ at 22 months that has the most genes shared with the 35 months old brain (112 genes in common) (**Fig. 4 B1 and Supp. Fig.1**). This similarity between the 2 month and 22 months *tert*$^{-/-}$, with the gut and brain, respectively, is also apparent when we just look at the pattern of the main hallmarks of ageing accelerated in the *tert*$^{-/-}$ (**Fig. 3, 4 and Graphical Abstract)**. Together, these data suggest that the gut is displaying telomerase-dependent hallmarks of ageing at an earlier age than the brain, consistent with what would be expected for a high *versus* low proliferative tissue. Of relevance, in the brain, of the genes de-regulated in the *tert*$^{-/-}$ 22 month that are in common with the WT aged at 35 months *ccna2* (cyclin a2), *cdk6* (cyclin-dependent kinase 6), *chek1 (*checkpoint kinase 1*), mad2l1(* Mitotic spindle assembly checkpoint protein mad2a*), tacc3 (*Transforming, acidic coiled-coil containing protein 3*), top2a (*DNA topoisomerase ii alpha*) and mcm2 (*DNA helicase, MCM2 minichromosome maintenance deficient 2*)* have also been included in the

Human Ageing Resources databases (Tacutu et al., 2018) and are mostly located within the same cluster (green), identified using *k-means* clustering in STRING analysis (Szklarczyk et al., 2021) (**Fig 4 and source data**). Of the proteins encoded by these genes, chek1 (Poehlmann et al., 2011), cdk6 (Morris, Hepburn, & Wynford-Thomas, 2002), mad2l1 (Lentini, Barra, Schillaci, & Di Leonardo, 2012) and tacc3 (Schmidt et al., 2010) have been reported to be involved in cellular senescence. Additionally, top2a has been involved in neuron proliferation (Watt & Hickson, 1994) and mcm2 depletion in mice leads to decreased proliferation in various tissue stem cell progenitors (Pruitt, Bailey, & Freeland, 2007).

2.4 Analysis of telomerase (*tert*)-dependent gene changes of old age

Once we identified what WT ageing looked like at the level of time-dependent gene expression changes over the life-course and the main biological processes affected, we sought to determine how much of these were likely to be telomerase-dependent. If a gene expression change or a biological process alteration is accelerated in the absence of telomerase (i.e becomes significant at an earlier age in the *tert*$^{-/-}$), we consider it to be telomerase dependent, as has been described before (Madalena C Carneiro et al., 2016; Henriques et al., 2013). Conversely, if none of these pre-requisites are met, we consider the gene/process alteration to be telomerase-independent. With this in mind we performed Venn diagrams (Oliveros, 2007-2015) to identify the telomerase-dependent significant gene alterations of old age, i.e, DEGs present in the WT at 35months old, when compared with the WT young control, i.e, at 2 months of age. For this, we used the DEGs identified in the STEM profiles (i.e., genes that change monotonically, in a time-dependent manner), combined with the more traditional DEG analysis, which include all gene changes, whether they change consistently in a time-dependent manner across the lifecourse or not (called "ALL DEGs" from hereafter) (**Fig. 5 and source data**). From these analyses, we identified 50 significant DEGs (out of 491; c. 10%) (present in old age (WT 35 months) that are prematurely de-regulated in the *tert*$^{-/-}$ gut (**Fig. 5 A**) and 100 genes (out of 428; c.23%) that are prematurely de-regulated in the *tert*$^{-/-}$ brain (**Fig. 5 B**). Importantly, most of these genes are directly or indirectly involved in known hallmarks of ageing (Lemoine, 2021; López-Otín et al., 2013), namely altered intercellular communication (including immunity,

inflammation, extra-cellular matrix), genome stability (including DNA replication and repair), stem cell exhaustion and mitochondrial dysfunction. In the gut, telomerase-dependent gene expression changes with ageing include up-regulation of genes involved in immune response, such as *tlr18 (Toll-like receptor 18 precursor), sytl1 (Synaptotagmin-like protein 1)* and down-regulation of genes involved in metabolism, such as *cyp8b1 (Cytochrome P450, family 8, subfamily B, polypeptide 1*) and *igfbp2a* (*Insulin-like growth factor-binding protein 2*) *(Bertaggia et al., 2017)*. Within the down-regulated genes, there are other well-known genes such as *sox6* (involved in stem cell function), vav3b (involved in wound healing), (**Fig 5 and source data**). Additionally, we identify a number of non-annotated genes, which may represent novel tert-dependent genes, that would require further investigation. Importantly, amongst these *tert*-dependent genes of "old age", there are a number of homolog or closely related genes which have been previously identified in ageing datasets (Tacutu et al., 2018) such as several *igfbps (insulin-like growth factor binding proteins), igf (insulin growth factor), mapks (mitogen-activated protein kinases), tlr3 (toll-like receptor 3) and nrg1 (neuroregulin 1).*

In the brain, *tert*-dependent ageing gene expression changes include mostly down-regulation of genes involved in cell cycle or neurogenesis, such as *aurkb (*aurora kinase B*), chek1 (*checkpoint kinase 1*), ccnb1 (*cyclin b1*), cdk2 (*cyclin-dependent kinase 2*)* and *neurod4 (*neuronal differentiation 4*), dld (delta d), nog1* (noggin 1), respectively, as well as genome stability and DNA repair, such as *rad54l (*rad54 like*), mcm5* (minichromosome maintenance complex component 5) and *smc4 (*structural maintenance of chromosomes 4*)*. Up-regulated genes are mostly involved in immune response or inflammation, such as *cxcl18b (*chemokine (C-X-C motif) ligand 18b*), mhc2a (*major histocompatibility complex class II integral membrane alpha chain gene*), socs1a (*suppressor of cytokine signalling 1a*), irf8 (*interferon regulatory factor 8*)* and *csf1b (*colony stimulating factor 1b (macrophage)*)*. Of note, amongst these *tert*-dependent DEGs of old age, we identified *dre-mir-29b-1*, which encodes for a regulatory micro RNA 29 (mir29), widely described to be up-regulated in ageing, in response to DNA damage, alongside P53 (Ugalde et al., 2011). mir29 up-regulation with ageing can act as a protective response, limiting excessive iron-exposure and damage in neurons (Ripa et al., 2017). As for the gut, there are a number of homolog or closely related genes which have been previously identified in ageing (Tacutu et al., 2018), such as *chek1*, *mad2l1 (*MAD2 mitotic arrest deficient-like 1 (yeast)*), dl3 (*delta like 3*), nog (*noggin*), ifnb1*

374 *(*interferon beta*), socs2 (*suppressor of cytokine signalling 2*,* amongst many others, which
375 can be found in the GeneAge database.

376 Since it is known that short telomeres themselves can lead to de-regulated gene
377 expression, particularly in genes near the chromosome ends due to loss of the "telomere
378 positioning effect" (TPE) (Robin et al., 2014), we proceeded to map the genes identified to
379 be de-regulated prematurely in the absence of telomerase to their chromosome location,
380 with the aim of determining whether they located to within up to 10MB of either of the
381 telomeric ends (**Fig. 5C1).** We found that whereas most tert-dependent gene changes of old
382 age do not locate to the end of chromosomes, in both gut and brain (**Fig. 5C2 and C3**).
383 However, there are significantly more *tert*-dependent genes located at the end of
384 chromosome in the gut than in the brain, (**Fig. 5 C4**). This is consistent with gut being a more
385 proliferative tissue, where telomeres are likely to shorten more, which would be particularly
386 exacerbated in the absence of *tert*, leading to a higher probability of TPE contributing to
387 gene transcription alterations.

388 **2.5 Transcriptional changes in common between the gut and brain at the early and**
389 **late stages of ageing**

390 Even though the aged phenotype is something usually observed late in life, the
391 underlying molecular and cellular mechanism driving these changes can, arguably, start
392 from the moment you are born (Gladyshev, 2021). To understand what significant
393 transcriptional changes are taking place in the gut and brain and, in particular, in common
394 between the gut and brain, we compared all DEGs and STEM DEGs in these tissues at the
395 earliest time point we detect significant changes (9 months) and at the late stages of ageing,
396 i.e, at the latest time point analysed of 35 months (**Fig 6, Supp Fig 3 and source data**). We
397 identified 7 gene changes in common between WT gut and brain at the early stages of
398 ageing (9 months of age). In specific, we identified 5 down-regulated genes, namely *ccnb1,*
399 *kif2c, serpinh1a, temem37* and *si:ch211-5k11.8*, and 2 up-regulated genes, namely *cfap45*
400 and *eif4ebp3l.* Of these, ccnb1 (G2/mitotic-specific cyclin-B1) and *kif2c* (Kinesin-like protein)
401 are both proteins involved in cell-cycle progression. Whereas *Ccnb1* has been reported to be
402 involved in normal stem-cell/progenitor maintenance in the brain (Hagey et al., 2020) and
403 gut (Basak et al., 2014); kif2c can act as a DNA damage repair protein, and, accordingly, its
404 depletion leads to significant accumulation of DNA damage (Zhu et al., 2020). STRING

analysis suggests these proteins are likely to be co-expressed in a variety of organisms including zebrafish and humans, highlighting potential functional links (**Fig 6 B and source data**). The downregulated *elf4ebp3l* gene (Eukaryotic translation initiation factor 4E-binding protein 3-like) encodes a repressor of translation and is inhibited in response to TORC1 (mammalian target of rapamycin complex 1) (Boutouja, Stiehm, & Platta, 2019).

At "late stages" of ageing, we identified 23 gene changes in common between the gut and brain. Of these, STRING analysis identified 2 main protein network interactions, namely a link between cd59 and cd99l2 and link between il2rb and b2m. In specific, cd59 and cd99l, which our data show to be downregulated in old age, in both gut and brain, have both been cited in the literature as markers of newborn neurons and oligodendrocyte progenitor cells, respectively, in a single-cell transcriptomic analysis of the adult zebrafish brain (Lange et al., 2020). In the gut, cd59, also known as protectin, has been shown to be downregulated in the gut epithelium of ulcerative colitis and Chron's disease patients and thought to render the tissue susceptible to inflammatory damage (Scheinin et al., 1999). cd99 has been shown to be a key molecule in modulating monocyte migration through endothelial junctions (Schenkel, Mamdouh, Chen, Liebman, & Muller, 2002) and monocyte differentiation to macrophages is known to be triggered by endothelial transmigration (Gerhardt & Ley, 2015; Li et al., 2020), including in the brain via migration through the blood-brain barrier (Ifergan et al., 2007). Il2rb and b2m, which our data show to be up-regulated in both gut and brain at the "late stages" of ageing, are key molecules involved in adaptive and innate immune function. Whilst the IL2R beta is important for T-cell mitogenic response to IL-2, the b2m (Beta-2-microglobulin) protein is a component of the major histocompatibility complex I (MHCI), involved in antigen presentation. Intriguingly, b2m has been shown to be present in a soluble free-form, and has been found to be systemically increased with ageing in humans and in individuals with neurodegenerative diseases (Smith et al., 2015). Importantly, heterochronic parabiosis experiments between young and old mice suggest that increased b2m with ageing leads to cognitive impairment and neurodegeneration, and has hence been identified as a systemic pro-ageing factor (Smith et al., 2015). Additionally, increased IL2 receptor expression has been shown to contribute to CD4 differentiation and exhaustion of their naïve pool and therefore ability to respond to infection with ageing, in humans (Pekalski et al., 2013; H. Zhang, Weyand, & Goronzy, 2021).

3 DISCUSSION

In this study, we used RNA sequencing analysis to determine the kinetics of telomerase-dependent and -independent transcriptomic changes occurring during WT ageing in brain and gut tissues, using the zebrafish as a model. We hypothesised that this would allow us to identify key age-associated genes and pathways that become prematurely de-regulated in both or either tissue, providing key insights into the early stages of ageing in each tissue and highlight potential interactions.

3.1 STEM versus all DEGs analysis

Ageing can be described as a time-dependent change in tissue homeostasis, that increases the probability of disease and death (Hayflick, 2007). Whether the genes and pathways driving these time-dependent changes are also consistently changing in a time-specific manner, remains unresolved. To account for both possibilities, we performed a time-series analysis (STEM) and then combined this with the more traditional differential gene expression (DEGs) analysis between young and old animals. Even though the gene changes identified with the STEM analysis were also picked up by the traditional DEGs analysis, the STEM analysis provided a much tighter, restrictive view of the transcriptomic signatures of ageing. In the gut, particularly, the main hallmarks of ageing identified using the STEM analysis are quite different from the ones using the traditional all DEGs. In particular, STEM analysis identifies mitochondrial dysfunction and de-regulated nutrient sensing as the main hallmarks of WT ageing at the earlier stages of ageing in the gut (WT 9 months), whereas all DEGs analysis identified stem cell dysfunction as the principal hallmark de-regulated at that age. The significance of these differences is difficult to judge, but it can suggest that changes in genes affecting mitochondrial function and nutrient sensing have a mostly monotonic trajectory in gut ageing, whereas the ones involved in stem cell maintenance can have different behaviours at different times throughout life. Nevertheless, this difference was not observed in the WT brain or in the *tert*$^{-/-}$ ageing, where STEM and all DEGs analysis led to very similar conclusions regarding the identity or kinetics of the main hallmarks of ageing affected. Importantly, the kinetics of gene changes and processes identified in our data match very well to the phenotypes of ageing previously reported in the *tert*$^{-/-}$ and WT ageing. In particular, in the gut, impaired cell proliferation in the gut is one

of the first *tert*-dependent phenotypes of ageing identified, followed by cellular senescence and inflammation later in life (Madalena C Carneiro et al., 2016; Henriques et al., 2013). Moreover, the recently reported *tert*-dependent changes in macrophage immune activation and increased gut permeability (Pam S. Ellis, 2022) are consistent with key tert-dependent gene changes of old age identified here. An example of such genes are *cd99*, potentially involved in macrophage differentiation via trans-endothelial migration (Gerhardt & Ley, 2015; Li et al., 2020; Schenkel et al., 2002); and *cldn5a* (claudin 5), involved in tight-junctions (Lu, Ding, Lu, & Chen, 2013).

3.2 Main hallmarks of ageing

A simplistic prediction of how the kinetics of the hallmarks of ageing would behave over the lifecourse could be that, at early ages, we would detect more changes affecting the primary hallmarks of ageing, i.e, the "causes of damage", namely genomic instability, telomere attrition, epigenetic alterations and loss of proteostasis. At the last stages, one could predict that we would detect more significant changes in the integrative hallmarks, i.e, the "culprits of the phenotype", namely stem cell exhaustion and altered intercellular communication, of which inflammation is a key component, as described in (López-Otín et al., 2013). However, either separately or combined, neither STEM nor all DEGs analysis show this. Our combined analyses show that most of the gene changes occurring at the early stages of WT ageing are observed from 9 months and are mostly involved in stem cell maintenance, in both gut and brain. One potential explanation for this observation is that our qualitative analysis was not able to distinguish between such hallmarks or is under-estimating the primary hallmarks. Another explanation comes from the relatively low sample size used for each time-point and the heterogeneity of individuals physiology amongst each population. As recently showed in (Dambroise et al., 2016), zebrafish age following the two-phase model first proposed flies (Tricoire & Rera, 2015), based on the age-related intestinal permeability assessed using the Smurf assay they previously described (Rera, Clark, & Walker, 2012). Moreover, we have recently shown that gut permeability with ageing, in zebrafish, is accelerated in the absence of telomerase ($tert^{-/-}$) (Pam S. Ellis, 2022). Following this model and considering the longevity curve from the population we sampled, the proportion of Smurfs might have been, approximately, <10% at 2 month, 25% at 9

month, 50% at 22 months and >80% at 35 months, based on previous work in flies (Rera et al., 2012). If we were to translate these findings to zebrafish, then the chances to have selected at least 1 Smurf by accident would be approximately 27% at 2 months, 57% at 9, 86% at 22 and 99% at 35%. This could contribute to the heterogeneity or potential bias towards having more of a specific ageing signature over another (Smurf versus non-Smurf).

At first glance, it is surprising that telomere dysfunction is not picked up as a main hallmark of ageing in the telomerase mutant model. However, this may simply be the reflection of the number of genes that have been directly implicated in each of these hallmarks. In specific, there are a lot less genes that one would identify as directly involved in telomere dysfunction, when compared to stem cell dysfunction, for example. The main culprits for telomere dysfunction would be telomerase and the shelterin components, whereas for stem cell dysfunction, all the cell cycle and DNA damage repair proteins can play a role. For example, *chek1, fxr1 and daxx*, which are all de-regulated in the old WT gut and brain (*chek1*) (**see source data**), have all been identified as potential regulators of telomeres (Nersisyan et al., 2019). Yet, because that is not the main function one would attribute to such genes, these would have been missed as part of the telomere dysfunction hallmark of ageing. Additionally, it is not possible to distinguish from just looking at lists of DEGs if such gene was de-regulated due to telomere dysfunction in the first place, or if its dysfunction will affect telomere function indirectly. These are some of the considerations that highlight the complexity of ageing and the non-linearity of how the hallmarks of ageing may drive ageing as well as each other and it is important to have them in mind when interpreting our analyses. Nevertheless, at the later stages of WT ageing (>35 months), altered intercellular communication, a previously described “culprit of the phenotype” is indeed the most significant hallmark of ageing detected in common between the gut and brain. Finally, in terms of the progression hallmarks of ageing, different hallmarks may play more prominent roles at specific times of life, and may be replaced by others at other times, explaining why we don’t necessarily always see a linear accumulation of the different hallmarks of ageing over-time. This is particularly evident in the gut, where stem cell exhaustion is the main hallmark identified by the combined STEM and ALL DEGs analysis, and it is barely represented at the later stages of life. In the brain, the progression seems to

529 be more linear, though, and most hallmarks present at the early time point of 9 months
530 remain until old age, when other hallmarks are further added.
531
532 **3.3 Telomerase- and/or telomere-dependent changes with ageing**
533 If a gene expression changes or a biological process alteration is accelerated in the
534 absence of telomerase (i.e becomes significant at an earlier age in the *tert*$^{-/-}$), we considered
535 it to be telomerase dependent. If we take a step back and look at the processes and, in turn,
536 hallmarks of ageing affected in the absence of telomerase, it becomes clear that the *tert*$^{-/-}$ is
537 indeed accelerating many of these changes. It is particularly evident when we look at the pie
538 charts depicting the different hallmarks of ageing affected at each time point in WT versus
539 *tert*$^{-/-}$. Here, it is striking how a 2-month-old *tert*$^{-/-}$ gut resembles a WT gut at the old age of
540 35 months, and how a 9- and 22-month-old *tert*$^{-/-}$ brain resembles an old WT brain at 35
541 months. This is further highlighted by the further comparison we performed, where we
542 asked at which age does the *tert*$^{-/-}$ share more gene expression changes with the WT old
543 (>35 months). In this analysis, we show that the 2 months old *tert*$^{-/-}$ has the most gene
544 expression changes shared with the 35 months old WT gut, whereas it is the *tert*$^{-/-}$ at 22
545 months that has the most gene expression changes shared with the 35 months old WT
546 brain. This suggests that the gut is displaying telomerase-dependent hallmarks of ageing at
547 an earlier age than the brain, which is consistent with what would be expected for a high
548 *versus* low proliferative tissue. Accordingly, when looking at the specific gene changes
549 accelerated in the absence of *tert*, i.e, we identify significantly more *tert*-dependent genes
550 located near the ends of chromosomes in the gut than in the brain, and therefore more
551 liable to have been altered due to telomere shortening. In the future, it would be insightful
552 to test how many of the *tert*-dependent gene changes occur due to non-canonical functions
553 of telomerase involved in transcriptional regulation.
554 Nevertheless, *tert*-dependent gene changes in both tissues are still a minority, serving
555 as a reminder that "all roads lead to Rome", and one should exercise caution when trying to
556 identify genes influencing the natural process of ageing using premature ageing models. It is
557 not necessarily the same genes influencing the processes of ageing in these models, even if
558 the processes and phenotypes are accelerated. We should also have this in mind when we
559 compare the sets of genes identified in this study with those previously identified as

implicated in human ageing, and not necessarily be surprised if only a small percentage of those are shared. One could argue that it is more important that the processes are shared. Nevertheless, we do identify many gene changes shared between zebrafish and human ageing databases as highlighted throughout the results' section.

3.4 Which genes to focus on if we were to target age-associated dysfunction in the gut and brain.

As a final step in our analysis, we wanted to identify common gene expression changes between the gut and the brain at the earliest stages of ageing, in our case, from the age of 9 months. We hypothesised that this may highlight potential common therapeutic targets for early intervention to prevent age-associated dysfunction in both tissues. We identified 7 significant DEGs in common between the gut and brain at 9 months of age, 5 down-regulated (*ccnb1, kif2c, serpinh1a, si:ch211-5k11.8 and tmem37*) and 2 up-regulated (*cfap45 and eif4ebp3l*). We could then hypothesise that restoring expression of these genes to youthful levels would have a positive impact on delaying or ameliorating the development of ageing phenotypes in both these tissues at the same time. Of note, we identified that, amongst these, *ccnb1* and *eif4ebp3l* were telomerase-dependent changes in the brain. If so, one could hypothesise that telomerase re-activation in the brain should restore these genes to young WT levels and potentially contribute to amelioration of *ccnb1*- and *eif4ebp3l*-dependent ageing phenotypes in the brain.

4 CONCLUSIONS

We provide the first systematic analysis of transcriptomic changes throughout the lifespan of zebrafish in the gut and brain of the same group of individuals, leading to the identification of key genes and processes likely involved in driving the ageing process in these tissues. Many of these genes have previously identified in human ageing databases and many of them are potentially new genes of ageing, which will have to be experimentally tested in relevant model organisms. This analysis and the open access availability of its source and raw data should provide a key steppingstone and framework supporting future work for understanding the ageing process and using zebrafish for studying ageing.

5 MATERIALS AND METHODS

5.1 Zebrafish husbandry, genotypes and ages

Zebrafish were maintained at the standard conditions of 27-28ºC, in a 14:10 hour light-dark cycle, and fed twice a day with *Artemia* (live rotifers) and Sparus (dry food). All the experiments were performed in the University of Sheffield. All animal work was approved by local animal review boards, including the Local Ethical Review Committee at the University of Sheffield (performed according to the protocols of Project Licence 70/8681).

Two strains of adult zebrafish (*Danio rerio*) were used for these studies: wild-type (WT; AB strain) and *tert*$^{-/-}$ (*tert*$^{AB/hu3430}$). Wild-type fish were obtained from the Zebrafish International Resource Center (ZIRC). The *telomerase* mutant line *tert*$^{AB/hu3430}$ was generated by *N*-ethyl-nitrosourea mutagenesis (Utrecht University, Netherlands(Wienholds et al., 2003)). It has a *T→A* point mutation in the *tert* gene and is available at the ZFIN repository, ZFIN ID: ZDB-GENO-100412–50, from ZIRC. The fish used in this study are direct descendants of the ones used previously[29,30], by which point it had been subsequently outcrossed five times with WT AB for clearing of potential background mutations derived from the random ENU mutagenesis from which this line was originated. The *tert*$^{hu3430/hu3430}$ homozygous mutant is referred to in the paper as *tert*$^{-/-}$ and was obtained by incrossing our *tert*$^{AB/hu3430}$ strain. Genotyping was performed by PCR of the *tert* gene[13,14]. In order to study age-related phenotypes in the zebrafish gut and brain, we used >30 months old fish for what we consider old in WT (in the last 25-30% of their lifespan), and we considered the *tert*$^{-/-}$ old fish at the equivalent age (>22 months), which approximately corresponds to the last 25-30% of their lifespan. In specific, 'Old' was defined as the age at which the majority of the fish present age-associated phenotypes, such as cachexia, loss of body mass and curvature of the spine. These phenotypes develop close to the time of death and are observed at >30 months of age in WT and at >22 months in *tert*$^{-/-}$(Madalena C Carneiro et al., 2016; Henriques et al., 2013).

5.2 Tissue dissection and RNA extraction

Animals from various age-groups were used for RNA-Sequencing (WT at 2, 9, 22 and >30 months of age; and *tert*$^{-/-}$ at 2, 9 and 22 months of age). Three biological replicates were used per group. Fish were culled by overdose of MS-222, followed by confirmation of death.

Then, the whole tissues were rapidly dissected in cold PBS (Sigma-Aldrich), transferred to a microcentrifuge tube containing 100 µl of Trizol (Thermo Fisher Scientific), snap-frozen in dry ice and stored at -80°. To isolate the RNA, extra 50 µl of Trizol was added to each sample, and the tissue was homogenized with a mechanical homogenizer (VWR International) and a 1.5 pestle (Kimble Chase, Vineland, NJ, USA). After 5 min incubation at room temperature (RT), 30 µl of chloroform (1:5, VWR International) was added and the samples were incubated for further 3 min at RT before centrifuged at 13,000g, for 30 min, at 4°C. Isopropanol (Thermo Fisher Scientific) was then added to the aqueous phase of the solution, and the resultant mix was incubated for 10 min at RT, before centrifuged (13,000g for 15 min at 4°C). Finally, the pellet was twice washed in 250 µl of ice cold 75% ethanol and left to air-dry, before resuspended in 14 µl of nuclease-free water. RNA integrity was assessed with the bioanalyzer Agilent 2100 Bioanalyzer (Agilent, Santa Clara, CA, USA). All the samples had a RNA integrity number (RIN) ≥9.

5.3 RNA-Sequencing

The RNA-Sequencing was performed at the *Genomics and Sequencing facility* of Sheffield Institute for Translational Neuroscience (SITraN). Library preparation was performed following the Illumina methodology. mRNA was extracted from 500 ng of RNA with oligo-dT beads, capturing poly(A) tails, using the NEBNext Poly(A) mRNA Magnetic Isolation Module (New England Biolabs Inc). cDNA libraries were made with the NEBNext® Ultra™ RNA Library Prep Kit for Illumina, following the manufacturer's instructions (New England Biolabs Inc). The samples were then sequenced on an Illumina HiSeq SQ, using a high output run and sequencing by synthesis V3 chemistry on a single 100 bp run. The data was imported into a FASTQ file format in order to perform the analysis.

5.4 RNA-Sequencing analysis

5.4.1 Data processing. Quality control was performed using MultiQC version 1.9. Cutadapt version 3.0 was used for trimming the first 13 bases from the reads to remove poor quality base pairs in the reads. Read alignment was performed as follows. Single-end reads were aligned against the reference genome Danio_rerio.GRCz11.dna. primary_assembly.fa using STAR. A bespoke alignment index was built using annotation file

Danio_rerio.GRCz11.103.gtf and an expected read length of 88 bp. Ht-seq count was run in non-stranded mode to obtain *per* gene read counts.

5.4.2 Differential expression. To identify signatures of ageing, WT gut and brain samples were subjected separately to DESEq2 analysis, comparing the time points 9, 22 and >30 months with the time-point of 2 months. Then, *tert*$^{-/-}$ samples at 2, 9 and 22 months were contrasted with WT at 2 months, in order to identify telomerase-dependent ageing processes.

5.4.3 Time-series analysis. Short Time-series Expression Miner (STEM) software was used to assign genes to predefined expression profiles genes based on their expression across the time points. For this, the 2 months' time-point was used as the zero time point for the analysis. The maximum number of model profiles was set to 50; the maximum unit change in model profiles between time points was set to 2; and the minimum absolute log ratio of expression was set to 1.0, with change based on maximum − minimum. Significance level of the model profiles was set to 0.05 with Bonferroni correction. Minimum correlation for profile clustering was set to 0.7. The statistically significant temporal profiles were visualised as line plots using ggplot2. Median expression fold change values of the genes in each profile were shown on the plots with a thicker line.

5.4.4 Enrichment analysis of temporal profiles from STEM. Enrichment analysis was performed using all the differentially expressed genes (DEGs) and using the genes identified in the STEM analysis, separately. Gee-set over-representation analysis (ORA) of GO Biological Process (GOBP), GO Molecular Function (GOMF), and GO Cellular Compartment (GOCC) terms were performed using the enrichGO function of clusterProfiler package version 3.18.0. Minimum and maximum gene set sizes were set to 10 and 500, respectively. Results were simplified using the simplify function of clusterProfiler with the similarity cut-off set to 0.7 and minimum adjusted p-value used as the feature for selecting the representative terms. Enrichment results with adjusted p-values below 0.05 and at least 3 core enrichment genes were considered significantly enriched. ORA of KEGG and REACTOME pathway terms were performed using the enrichKEGG and enrichPathway functions of clusterProfiler. Minimum and maximum gene set sizes were set to 10 and 500, respectively. The same significance criteria for the enrichments were used as for the GO term enrichments. Results of the enrichment results were visualised as barplots or as pie

charts. Barplots were made using the ggbarplot function of R package (R studio version 2021.09.2), ggpubr version 0.4.0, showing a maximum of five pathways with adjusted p-value below 0.05 *per* pathway category. Pie charts were made using Prism GraphPad version 9.0.

5.4.5 Protein-protein interaction network analysis

The search tool for retrieval of interacting genes (STRING) (https://string-db.org) database, which integrates both known and predicted PPIs, was used to predict functional interactions of proteins(Szklarczyk et al., 2021). Active interaction sources, including text mining, experiments, databases, and co-expression as well as species limited to "Danio rerio" and an interaction score > 0.7 (high confidence) were applied to construct the PPI networks. The network was further clustered using *k-means* clustering to a specific number of up to 3 clusters.

5.4.6 Venn Diagram analysis

Venn Diagram analysis was performed using the online tool Venny 2.1.0 – BioinfoGP (https://bioinfogp.cnb.csic.es/tools/venny/)(Oliveros, 2007-2015).

5.4.7 Statistical analysis

A chi-square test was used in **Fig 5** to compare between the relative chromosome location of telomerase-dependent genes in the gut and brain, using raw data values, even though it is the % that is represented in the graphs, to ensure accurate analysis. P value <0.05 was considered significant and denoted with a *, whereas ns was used to denote non-significant differences.

ACKNOWLEDGEMENTS

The authors would like to acknowledge Genevia Technologies Oy for the main bulk of RNA sequencing analysis service. We are very grateful to Joao Ribeiro for valuable advice regarding the many functionalities of Microsoft Excel, which greatly facilitated data analysis. This work was generously funded by a University of Sheffield PhD studentship to RRM, a Sheffield University Vice Chancellor's Research Fellowship and a Wellcome Trust/Royal Society Sir Henry Dale Fellowship (UNS35121) to CMH. Michael Rera is supported by CNRS.

AUTHOR CONTRIBUTIONS

RRM and CMH conceived and designed this work; RRM performed additional RNA sequencing beyond that provided by Genevia services; RRM, MR and CMH analysed and interpreted RNA sequencing results and co-wrote the manuscript; CMH designed the figures with input from co-authors.

COMPETING INTERESTS

The authors declare no competing interests

DATA AVAILABILITY STATEMENT

The RNA sequencing data from this experiment were deposited in gene expression omnibus (GEO) and will be made available when in peer review.

ORCID

Raquel Rua Martins: https://orcid.org/0000-0003-3952-8649

Michael Rera: https://orcid.org/0000-0002-6574-6511

Catarina Martins Henriques: https://orcid.org/0000-0003-1882-756X

SUPPORTING INFORMATION

Supporting information in the form of figures, tables and source data can be found online in the Supportive information section at the end of the article

REFERENCES

Ahmed, S., Passos, J. F., Birket, M. J., Beckmann, T., Brings, S., Peters, H., . . . Saretzki, G. (2008). Telomerase does not counteract telomere shortening but protects mitochondrial function under oxidative stress. *J Cell Sci, 121*(Pt 7), 1046-1053. doi:10.1242/jcs.019372

744 Anchelin, M., Alcaraz-Perez, F., Martinez, C. M., Bernabe-Garcia, M., Mulero, V., & Cayuela,
745 M. L. (2013). Premature aging in telomerase-deficient zebrafish. *Dis Model Mech,*
746 *6*(5), 1101-1112. doi:10.1242/dmm.011635
747 Baker, D. J., Childs, B. G., Durik, M., Wijers, M. E., Sieben, C. J., Zhong, J., . . . van Deursen, J.
748 M. (2016). Naturally occurring p16(Ink4a)-positive cells shorten healthy lifespan.
749 *Nature, 530*(7589), 184-189. doi:10.1038/nature16932
750 Baker, D. J., Wijshake, T., Tchkonia, T., LeBrasseur, N. K., Childs, B. G., van de Sluis, B., . . .
751 van Deursen, J. M. (2011). Clearance of p16Ink4a-positive senescent cells delays
752 ageing-associated disorders. *Nature, 479*(7372), 232-236. doi:10.1038/nature10600
753 Basak, O., van de Born, M., Korving, J., Beumer, J., van der Elst, S., van Es, J. H., & Clevers, H.
754 (2014). Mapping early fate determination in Lgr5+ crypt stem cells using a novel
755 Ki67-RFP allele. *EMBO J, 33*(18), 2057-2068. doi:10.15252/embj.201488017
756 Bertaggia, E., Jensen, K. K., Castro-Perez, J., Xu, Y., Di Paolo, G., Chan, R. B., . . . Haeusler, R.
757 A. (2017). Cyp8b1 ablation prevents Western diet-induced weight gain and hepatic
758 steatosis because of impaired fat absorption. *Am J Physiol Endocrinol Metab, 313*(2),
759 E121-E133. doi:10.1152/ajpendo.00409.2016
760 Blackburn, E. H., Epel, E. S., & Lin, J. (2015). Human telomere biology: A contributory and
761 interactive factor in aging, disease risks, and protection. *Science, 350*, 1193-1198.
762 doi:10.1126/science.aab3389
763 Bodnar, A. G. (1998). Extension of Life-Span by Introduction of Telomerase into Normal
764 Human Cells. *Science, 279*(5349), 349-352. doi:10.1126/science.279.5349.349
765 Boutouja, F., Stiehm, C. M., & Platta, H. W. (2019). mTOR: A Cellular Regulator Interface in
766 Health and Disease. *Cells, 8*(1). doi:10.3390/cells8010018
767 Cao, Y., Li, H., Deb, S., & Liu, J. P. (2002). TERT regulates cell survival independent of
768 telomerase enzymatic activity. *Oncogene, 21*(20), 3130-3138.
769 doi:10.1038/sj.onc.1205419
770 Cardoso, B. a., Gírio, a., Henriques, C., Martins, L. R., Santos, C., Silva, a., & Barata, J. T.
771 (2008). Aberrant signaling in T-cell acute lymphoblastic leukemia: Biological and
772 therapeutic implications. *Brazilian Journal of Medical and Biological Research, 41*,
773 344-350. doi:10.1590/S0100-879X2008005000016
774 Carneiro, M. C., de Castro, I. P., & Ferreira, M. G. (2016). Telomeres in aging and disease:
775 lessons from zebrafish. *Dis Model Mech, 9*(7), 737-748. doi:10.1242/dmm.025130
776 Carneiro, M. C., Henriques, C. M., Nabais, J., Ferreira, T., Carvalho, T., & Ferreira, M. G.
777 (2016). Short Telomeres in Key Tissues Initiate Local and Systemic Aging in Zebrafish.
778 *PLoS Genet, 12*, e1005798. doi:10.1371/journal.pgen.1005798
779 Choi, J., Southworth, L. K., Sarin, K. Y., Venteicher, A. S., Ma, W., Chang, W., . . . Artandi, S. E.
780 (2008). TERT promotes epithelial proliferation through transcriptional control of a
781 Myc- and Wnt-related developmental program. *PLoS Genet, 4*(1), e10.
782 doi:10.1371/journal.pgen.0040010
783 d'Adda di Fagagna, F., Reaper, P. M., Clay-Farrace, L., Fiegler, H., Carr, P., Von Zglinicki, T., . .
784 . Jackson, S. P. (2003). A DNA damage checkpoint response in telomere-initiated
785 senescence. *Nature, 426*(6963), 194-198. doi:10.1038/nature02118
786 Dambroise, E., Monnier, L., Ruisheng, L., Aguilaniu, H., Joly, J. S., Tricoire, H., & Rera, M.
787 (2016). Two phases of aging separated by the Smurf transition as a public path to
788 death. *Sci Rep, 6*, 23523. doi:10.1038/srep23523

De Felice, B., Annunziata, A., Fiorentino, G., Manfellotto, F., D'Alessandro, R., Marino, R., . . . Biffali, E. (2014). Telomerase expression in amyotrophic lateral sclerosis (ALS) patients. *J Hum Genet, 59*(10), 555-561. doi:10.1038/jhg.2014.72

de Jong, P. R., Gonzalez-Navajas, J. M., & Jansen, N. J. (2016). The digestive tract as the origin of systemic inflammation. *Crit Care, 20*(1), 279. doi:10.1186/s13054-016-1458-3

de Lange, T. (2004). T-loops and the origin of telomeres. *Nature reviews. Molecular cell biology, 5*, 323-329. doi:10.1038/nrm1422

Deacon, K., & Knox, A. J. (2018). PINX1 and TERT Are Required for TNF-alpha-Induced Airway Smooth Muscle Chemokine Gene Expression. *J Immunol, 200*(4), 1283-1294. doi:10.4049/jimmunol.1700414

Dimri, G. P., Lee, X., Basile, G., Acosta, M., Scott, G., Roskelley, C., . . . et al. (1995). A biomarker that identifies senescent human cells in culture and in aging skin in vivo. *Proc Natl Acad Sci U S A, 92*(20), 9363-9367.

Eitan, E., Tichon, A., Gazit, A., Gitler, D., Slavin, S., & Priel, E. (2012). Novel telomerase-increasing compound in mouse brain delays the onset of amyotrophic lateral sclerosis. *EMBO Mol Med, 4*(4), 313-329. doi:10.1002/emmm.201200212

England, P. H. (2017). *Chapter 1: life expectancy and healthy life expectancy*. Retrieved from https://www.gov.uk/government/publications/health-profile-for-england/chapter-1-life-expectancy-and-healthy-life-expectancy#references.

Ernst, J., & Bar-Joseph, Z. (2006). STEM: a tool for the analysis of short time series gene expression data. *BMC Bioinformatics, 7*, 191. doi:10.1186/1471-2105-7-191

Ferreira, M. G., Miller, K. M., & Cooper, J. P. (2004). Indecent exposure: when telomeres become uncapped. *Mol Cell, 13*(1), 7-18.

Forsyth, N. R., Wright, W. E., & Shay, J. W. (2002). Telomerase and differentiation in multicellular organisms: turn it off, turn it on, and turn it off again. *Differentiation, 69*(4-5), 188-197. doi:10.1046/j.1432-0436.2002.690412.x

Gerhardt, T., & Ley, K. (2015). Monocyte trafficking across the vessel wall. *Cardiovascular Research, 107*(3), 321-330. doi:10.1093/cvr/cvv147

Ghosh, A., Saginc, G., Leow, S. C., Khattar, E., Shin, E. M., Yan, T. D., . . . Tergaonkar, V. (2012). Telomerase directly regulates NF-kappaB-dependent transcription. *Nat Cell Biol, 14*(12), 1270-1281. doi:10.1038/ncb2621

Gladyshev, V. N. (2021). The Ground Zero of Organismal Life and Aging. *Trends Mol Med, 27*(1), 11-19. doi:10.1016/j.molmed.2020.08.012

Gomes, N. M. V., Ryder, O. a., Houck, M. L., Charter, S. J., Walker, W., Forsyth, N. R., . . . Wright, W. E. (2011). Comparative biology of mammalian telomeres: hypotheses on ancestral states and the roles of telomeres in longevity determination. *Aging Cell, 10*, 761-768. doi:10.1111/j.1474-9726.2011.00718.x

Goodman, W. A., & Jain, M. K. (2011). Length does not matter: A new take on telomerase reverse transcriptase. *Arteriosclerosis, thrombosis, and vascular biology, 31*, 235-236. doi:10.1161/ATVBAHA.110.220343

Greider, C. W., & Blackburn, E. H. (1985). Identification of a specific telomere terminal transferase activity in Tetrahymena extracts. *Cell, 43*(2 Pt 1), 405-413. doi:10.1016/0092-8674(85)90170-9

Haendeler, J., Drose, S., Buchner, N., Jakob, S., Altschmied, J., Goy, C., . . . Dimmeler, S. (2009). Mitochondrial telomerase reverse transcriptase binds to and protects

mitochondrial DNA and function from damage. *Arterioscler Thromb Vasc Biol, 29*(6), 929-935. doi:10.1161/ATVBAHA.109.185546

Hagey, D. W., Topcic, D., Kee, N., Reynaud, F., Bergsland, M., Perlmann, T., & Muhr, J. (2020). CYCLIN-B1/2 and -D1 act in opposition to coordinate cortical progenitor self-renewal and lineage commitment. *Nat Commun, 11*(1), 2898. doi:10.1038/s41467-020-16597-8

Hayflick, L. (2007). Biological aging is no longer an unsolved problem. *Ann N Y Acad Sci, 1100*, 1-13. doi:10.1196/annals.1395.001

Henriques, C. M., Carneiro, M. C., Tenente, I. M., Jacinto, A., & Ferreira, M. G. (2013). Telomerase is required for zebrafish lifespan. *PLoS Genet, 9*(1), e1003214. doi:10.1371/journal.pgen.1003214

Henriques, C. M., & Ferreira, M. G. (2012). Consequences of telomere shortening during lifespan. *Curr Opin Cell Biol, 24*(6), 804-808. doi:10.1016/j.ceb.2012.09.007

Hong, S. N., Joung, J. G., Bae, J. S., Lee, C. S., Koo, J. S., Park, S. J., . . . Kim, Y. H. (2017). RNA-seq Reveals Transcriptomic Differences in Inflamed and Noninflamed Intestinal Mucosa of Crohn's Disease Patients Compared with Normal Mucosa of Healthy Controls. *Inflamm Bowel Dis, 23*(7), 1098-1108. doi:10.1097/MIB.0000000000001066

Ifergan, I., Kébir, H., Bernard, M., Wosik, K., Dodelet-Devillers, A., Cayrol, R., . . . Prat, A. (2007). The blood–brain barrier induces differentiation of migrating monocytes into Th17-polarizing dendritic cells. *Brain, 131*(3), 785-799. doi:10.1093/brain/awm295

Jaskelioff, M., Muller, F. L., Paik, J.-H., Thomas, E., Jiang, S., Adams, A. C., . . . Depinho, R. a. (2011). Telomerase reactivation reverses tissue degeneration in aged telomerase-deficient mice. *Nature, 469*, 102-106. doi:10.1038/nature09603

Jurk, D., Wang, C., Miwa, S., Maddick, M., Korolchuk, V., Tsolou, A., . . . von Zglinicki, T. (2012). Postmitotic neurons develop a p21-dependent senescence-like phenotype driven by a DNA damage response. *Aging Cell, 11*(6), 996-1004. doi:10.1111/j.1474-9726.2012.00870.x

Lange, C., Rost, F., Machate, A., Reinhardt, S., Lesche, M., Weber, A., . . . Brand, M. (2020). Single cell sequencing of radial glia progeny reveals the diversity of newborn neurons in the adult zebrafish brain. *Development, 147*(1). doi:10.1242/dev.185595

Lawson, N. D., Li, R., Shin, M., Grosse, A., Yukselen, O., Stone, O. A., . . . Zhu, L. (2020). An improved zebrafish transcriptome annotation for sensitive and comprehensive detection of cell type-specific genes. *Elife, 9*. doi:10.7554/eLife.55792

Lee, H. W., Blasco, M. A., Gottlieb, G. J., Horner, J. W., 2nd, Greider, C. W., & DePinho, R. A. (1998). Essential role of mouse telomerase in highly proliferative organs. *Nature, 392*(6676), 569-574. doi:10.1038/33345

Lee, J., Jo, Y. S., Sung, Y. H., Hwang, I. K., Kim, H., Kim, S. Y., . . . Lee, H. W. (2010). Telomerase deficiency affects normal brain functions in mice. *Neurochem Res, 35*(2), 211-218. doi:10.1007/s11064-009-0044-3

Lemoine, M. (2021). The Evolution of the Hallmarks of Aging. *Front Genet, 12*, 693071. doi:10.3389/fgene.2021.693071

Lentini, L., Barra, V., Schillaci, T., & Di Leonardo, A. (2012). MAD2 depletion triggers premature cellular senescence in human primary fibroblasts by activating a p53 pathway preventing aneuploid cells propagation. *J Cell Physiol, 227*(9), 3324-3332. doi:10.1002/jcp.24030

881 Li, L., Song, J., Chuquisana, O., Hannocks, M. J., Loismann, S., Vogl, T., . . . Sorokin, L. (2020).
882 Endothelial Basement Membrane Laminins as an Environmental Cue in Monocyte
883 Differentiation to Macrophages. *Front Immunol, 11*, 584229.
884 doi:10.3389/fimmu.2020.584229
885 The hallmarks of aging, 153 (2013).
886 Lu, Z., Ding, L., Lu, Q., & Chen, Y. H. (2013). Claudins in intestines: Distribution and functional
887 significance in health and diseases. *Tissue Barriers, 1*(3), e24978.
888 doi:10.4161/tisb.24978
889 Mattiussi, M., Tilman, G., Lenglez, S., & Decottignies, A. (2012). Human telomerase
890 represses ROS-dependent cellular responses to Tumor Necrosis Factor-α without
891 affecting NF-κB activation. *Cellular signalling, 24*, 708-717.
892 doi:10.1016/j.cellsig.2011.11.004
893 Morris, M., Hepburn, P., & Wynford-Thomas, D. (2002). Sequential extension of proliferative
894 lifespan in human fibroblasts induced by over-expression of CDK4 or 6 and loss of
895 p53 function. *Oncogene, 21*(27), 4277-4288. doi:10.1038/sj.onc.1205492
896 Neale, B. M., Fagerness, J., Reynolds, R., Sobrin, L., Parker, M., Raychaudhuri, S., . . . Seddon,
897 J. M. (2010). Genome-wide association study of advanced age-related macular
898 degeneration identifies a role of the hepatic lipase gene (LIPC). *Proc Natl Acad Sci U S*
899 *A, 107*(16), 7395-7400. doi:10.1073/pnas.0912019107
900 Nersisyan, L., Hopp, L., Loeffler-Wirth, H., Galle, J., Loeffler, M., Arakelyan, A., & Binder, H.
901 (2019). Telomere Length Maintenance and Its Transcriptional Regulation in Lynch
902 Syndrome and Sporadic Colorectal Carcinoma. *Front Oncol, 9*, 1172.
903 doi:10.3389/fonc.2019.01172
904 Oliveros, J. C. (2007-2015). Venny. An interactive tool for comparing lists with Venn's
905 diagrams. Retrieved from https://bioinfogp.cnb.csic.es/tools/venny/index.html
906 Ovadya, Y., & Krizhanovsky, V. (2014). Senescent cells: SASPected drivers of age-related
907 pathologies. *Biogerontology, 15*, 627-642. doi:10.1007/s10522-014-9529-9
908 Pam S. Ellis, R. R. M., Emily J. Thompson, Asma Farhat, Stephen A. Renshaw, Catarina M.
909 Henriques. (2022). *A subset of gut leukocytes have telomerase-dependent "hyper-*
910 *long" telomeres and require telomerase for function in zebrafish*. Biorxiv.
911 Pekalski, M. L., Ferreira, R. C., Coulson, R. M., Cutler, A. J., Guo, H., Smyth, D. J., . . . Wicker,
912 L. S. (2013). Postthymic expansion in human CD4 naive T cells defined by expression
913 of functional high-affinity IL-2 receptors. *J Immunol, 190*(6), 2554-2566.
914 doi:10.4049/jimmunol.1202914
915 Poehlmann, A., Habold, C., Walluscheck, D., Reissig, K., Bajbouj, K., Ullrich, O., . . . Schneider-
916 Stock, R. (2011). Cutting edge: Chk1 directs senescence and mitotic catastrophe in
917 recovery from G(2) checkpoint arrest. *J Cell Mol Med, 15*(7), 1528-1541.
918 doi:10.1111/j.1582-4934.2010.01143.x
919 Pruitt, S. C., Bailey, K. J., & Freeland, A. (2007). Reduced Mcm2 expression results in severe
920 stem/progenitor cell deficiency and cancer. *Stem Cells, 25*(12), 3121-3132.
921 doi:10.1634/stemcells.2007-0483
922 Rahman, R., Latonen, L., & Wiman, K. G. (2005). hTERT antagonizes p53-induced apoptosis
923 independently of telomerase activity. *Oncogene, 24*(8), 1320-1327.
924 doi:10.1038/sj.onc.1208232
925 Raj, D. D. A., Moser, J., van der Pol, S. M. A., van Os, R. P., Holtman, I. R., Brouwer, N., . . .
926 Boddeke, H. W. G. M. (2015). Enhanced microglial pro-inflammatory response to
927 lipopolysaccharide correlates with brain infiltration and blood-brain barrier

928 dysregulation in a mouse model of telomere shortening. *Aging Cell*, 1003-1013.
929 doi:10.1111/acel.12370
930 Rando, T. A., & Wyss-Coray, T. (2021). Asynchronous, contagious and digital aging. *Nat*
931 *Aging, 1*(1), 29-35. doi:10.1038/s43587-020-00015-1
932 Rera, M., Azizi, M. J., & Walker, D. W. (2013). Organ-specific mediation of lifespan extension:
933 more than a gut feeling? *Ageing Res Rev, 12*(1), 436-444.
934 doi:10.1016/j.arr.2012.05.003
935 Rera, M., Clark, R. I., & Walker, D. W. (2012). Intestinal barrier dysfunction links metabolic
936 and inflammatory markers of aging to death in Drosophila. *Proc Natl Acad Sci U S A,*
937 *109*(52), 21528-21533. doi:10.1073/pnas.1215849110
938 Ripa, R., Dolfi, L., Terrigno, M., Pandolfini, L., Savino, A., Arcucci, V., . . . Cellerino, A. (2017).
939 MicroRNA miR-29 controls a compensatory response to limit neuronal iron
940 accumulation during adult life and aging. *BMC Biol, 15*(1), 9. doi:10.1186/s12915-
941 017-0354-x
942 Robin, J. D., Ludlow, A. T., Batten, K., Magdinier, F., Stadler, G., Wagner, K. R., . . . Wright, W.
943 E. (2014). Telomere position effect: regulation of gene expression with progressive
944 telomere shortening over long distances. *Genes Dev, 28*(22), 2464-2476.
945 doi:10.1101/gad.251041.114
946 Romaniuk, A., Paszel-Jaworska, A., Toton, E., Lisiak, N., Holysz, H., Krolak, A., . . . Rubis, B.
947 (2018). The non-canonical functions of telomerase: to turn off or not to turn off. *Mol*
948 *Biol Rep*. doi:10.1007/s11033-018-4496-x
949 Rudnicka, E., Napierala, P., Podfigurna, A., Meczekalski, B., Smolarczyk, R., & Grymowicz, M.
950 (2020). The World Health Organization (WHO) approach to healthy ageing.
951 *Maturitas, 139*, 6-11. doi:10.1016/j.maturitas.2020.05.018
952 Santamarina-Fojo, S., Gonzalez-Navarro, H., Freeman, L., Wagner, E., & Nong, Z. (2004).
953 Hepatic lipase, lipoprotein metabolism, and atherogenesis. *Arterioscler Thromb Vasc*
954 *Biol, 24*(10), 1750-1754. doi:10.1161/01.ATV.0000140818.00570.2d
955 Sarin, K. Y., Cheung, P., Gilison, D., Lee, E., Tennen, R. I., Wang, E., . . . Artandi, S. E. (2005).
956 Conditional telomerase induction causes proliferation of hair follicle stem cells.
957 *Nature, 436*(7053), 1048-1052. doi:10.1038/nature03836
958 Schaum, N., Lehallier, B., Hahn, O., Palovics, R., Hosseinzadeh, S., Lee, S. E., . . . Wyss-Coray,
959 T. (2020). Ageing hallmarks exhibit organ-specific temporal signatures. *Nature,*
960 *583*(7817), 596-602. doi:10.1038/s41586-020-2499-y
961 Scheinin, T., Bohling, T., Halme, L., Kontiainen, S., Bjorge, L., & Meri, S. (1999). Decreased
962 expression of protectin (CD59) in gut epithelium in ulcerative colitis and Crohn's
963 disease. *Hum Pathol, 30*(12), 1427-1430. doi:10.1016/s0046-8177(99)90163-6
964 Schenkel, A. R., Mamdouh, Z., Chen, X., Liebman, R. M., & Muller, W. A. (2002). CD99 plays a
965 major role in the migration of monocytes through endothelial junctions. *Nature*
966 *immunology, 3*(2), 143-150. doi:10.1038/ni749
967 Schmidt, S., Schneider, L., Essmann, F., Cirstea, I. C., Kuck, F., Kletke, A., . . . Piekorz, R. P.
968 (2010). The centrosomal protein TACC3 controls paclitaxel sensitivity by modulating
969 a premature senescence program. *Oncogene, 29*(46), 6184-6192.
970 doi:10.1038/onc.2010.354
971 Segal-Bendirdjian, E., & Geli, V. (2019). Non-canonical Roles of Telomerase: Unraveling the
972 Imbroglio. *Front Cell Dev Biol, 7*, 332. doi:10.3389/fcell.2019.00332
973 Shokhirev, M. N., & Johnson, A. A. (2021). Modeling the human aging transcriptome across
974 tissues, health status, and sex. *Aging Cell, 20*(1), e13280. doi:10.1111/acel.13280

Smith, L. K., He, Y., Park, J. S., Bieri, G., Snethlage, C. E., Lin, K., . . . Villeda, S. A. (2015). beta2-microglobulin is a systemic pro-aging factor that impairs cognitive function and neurogenesis. *Nat Med, 21*(8), 932-937. doi:10.1038/nm.3898

Spilsbury, A., Miwa, S., Attems, J., & Saretzki, G. (2015). The role of telomerase protein TERT in Alzheimer's disease and in tau-related pathology in vitro. *J Neurosci, 35*(4), 1659-1674. doi:10.1523/JNEUROSCI.2925-14.2015

Sullivan, D. I., Jiang, M., Hinchie, A. M., Roth, M. G., Bahudhanapati, H., Nouraie, M., . . . Alder, J. K. (2021). Transcriptional and Proteomic Characterization of Telomere-Induced Senescence in a Human Alveolar Epithelial Cell Line. *Front Med (Lausanne), 8*, 600626. doi:10.3389/fmed.2021.600626

Sung, Y. H., Ali, M., & Lee, H. W. (2014). Extracting extra-telomeric phenotypes from telomerase mouse models. *Yonsei Medical Journal, 55*, 1-8. doi:10.3349/ymj.2014.55.1.1

Szklarczyk, D., Gable, A. L., Nastou, K. C., Lyon, D., Kirsch, R., Pyysalo, S., . . . von Mering, C. (2021). The STRING database in 2021: customizable protein-protein networks, and functional characterization of user-uploaded gene/measurement sets. *Nucleic Acids Res, 49*(D1), D605-D612. doi:10.1093/nar/gkaa1074

Tabula Muris, C. (2020). A single-cell transcriptomic atlas characterizes ageing tissues in the mouse. *Nature, 583*(7817), 590-595. doi:10.1038/s41586-020-2496-1

Tacutu, R., Thornton, D., Johnson, E., Budovsky, A., Barardo, D., Craig, T., . . . de Magalhaes, J. P. (2018). Human Ageing Genomic Resources: new and updated databases. *Nucleic Acids Res, 46*(D1), D1083-D1090. doi:10.1093/nar/gkx1042

Tricoire, H., & Rera, M. (2015). A New, Discontinuous 2 Phases of Aging Model: Lessons from Drosophila melanogaster. *PLoS One, 10*(11), e0141920. doi:10.1371/journal.pone.0141920

Ugalde, A. P., Ramsay, A. J., de la Rosa, J., Varela, I., Marino, G., Cadinanos, J., . . . Lopez-Otin, C. (2011). Aging and chronic DNA damage response activate a regulatory pathway involving miR-29 and p53. *EMBO J, 30*(11), 2219-2232. doi:10.1038/emboj.2011.124

Watt, P. M., & Hickson, I. D. (1994). Structure and function of type II DNA topoisomerases. *Biochem J, 303 (Pt 3)*, 681-695. doi:10.1042/bj3030681

Wienholds, E., van Eeden, F., Kosters, M., Mudde, J., Plasterk, R. H., & Cuppen, E. (2003). Efficient target-selected mutagenesis in zebrafish. *Genome Res, 13*(12), 2700-2707. doi:10.1101/gr.1725103

Zhang, H., Weyand, C. M., & Goronzy, J. J. (2021). Hallmarks of the aging T-cell system. *FEBS J, 288*(24), 7123-7142. doi:10.1111/febs.15770

Zhang, M. J., Pisco, A. O., Darmanis, S., & Zou, J. (2021). Mouse aging cell atlas analysis reveals global and cell type-specific aging signatures. *Elife, 10*. doi:10.7554/eLife.62293

Zhao, Y., Hasse, S., & Bourgoin, S. G. (2021). Phosphatidylserine-specific phospholipase A1: A friend or the devil in disguise. *Prog Lipid Res, 83*, 101112. doi:10.1016/j.plipres.2021.101112

Zhu, S., Paydar, M., Wang, F., Li, Y., Wang, L., Barrette, B., . . . Peng, A. (2020). Kinesin Kif2C in regulation of DNA double strand break dynamics and repair. *Elife, 9*. doi:10.7554/eLife.53402

FIGURE LEGENDS

Graphical Abstract: Telomerase depletion accelerates the appearance of hallmark of ageing in both gut and brain. In specific, the *tert*$^{-/-}$ gut at 2 months shows similar hallmarks of ageing as the WT old gut, whereas the brain *tert*$^{-/-}$ brain only *starts* displaying similar hallmarks of ageing as the WT old brain from the age of 9 months. We identified stem cell exhaustion is the common principal hallmark of ageing at the early stages of ageing, in both tissues. Finally, we further identified altered intercellular communication as the main telomerase-dependent hallmark of ageing common between the gut and brain.

Fig 1. Summary of the experimental design and principal component analysis (PCA). (A) RNA-Sequencing was performed in whole gut and brain tissues from WT and *tert*$^{-/-}$ zebrafish, at different timepoints throughout their lifespan. Age-associated transcriptomic changes were analysed using two different methods: time-series analysis (genes that change consistently overtime) and all differentially expressed genes (ALL DEGs; genes whose expression is altered over-time, in both genotypes, as compared with the WT young baseline. (B) PCA representing the variation in the data from gut (gold) and brain (pink) tissues, in both WT and *tert*$^{-/-}$ fish. (C-D) PCA showing the variation in the data from fish at different ages (2 months, pink; 9 months, green; 22 months, blue; 35 months, purple), in WT (circle) versus *tert*$^{-/-}$ fish (triangle), in (C) gut and (D) brain samples. PCA was performed using the plotPCA function of DESeq2 and considering the top 500 genes with highest variance across the samples. (E) Summary of the number of significantly de-regulated genes at each time-point, in both genotypes, in gut (E1) and brain (E2) tissues, over-time, as compared with the WT young baseline.

Fig 2. Identification of time-dependent signatures of ageing in the WT and *tert*$^{-/-}$ zebrafish gut and brain. (A, B) Transcriptomic temporal profiles in the (A) gut and brain (B) of WT (black) and *tert*$^{-/-}$ fish (red) were identified using the Short Time-series Expression Miner (STEM) and are represented in line plots. The thicker lines on the plots represent the median fold change of each profile. For each temporal profile, enrichment analysis was

performed using the enrichGO, enrichKEGG, and enrichPathway functions of clusterProfiler package version 3.18.0. Processes and pathways from each temporal profile were further classified and grouped according to the main hallmarks of ageing (Lemoine, 2021; López-Otín et al., 2013), which is represented in pie charts. (A1, B1) A summary of the enrichment analysis of one of the profiles is represented in the bar plots, where processes and pathways are represented in different colours according to the classification into hallmarks of ageing. This summary contains the top enriched processes and pathways from each database (p-value >0.05 and at least 3 core enrichment genes; up to 5 terms *per* database: GOBP, GOCC, GOMF, KEEG, and REACTOME).

Fig 3. Qualitative changes in the hallmarks of ageing over-time, comparing WT and *tert*$^{-/-}$ zebrafish gut and brain. The age-associated enriched processes and pathways identified in the previous figures were further re-classified and grouped into the main well-known hallmarks of ageing. (A-B) Pie charts represent the hallmarks of ageing identified in the (A) gut and (B) brain, at different ages throughout WT (black) and *tert*$^{-/-}$ (red) zebrafish lifespan. This analysis was performed considering the (A1, B1) genes identified in the temporal profiles (within STEM), (A2, B2) all the genes differentially expressed at any timepoint (within ALL DEGs), and (A3, B3) STEM and ALL DEGs combined. (A4, B4) The number of transcriptomic changes increases with ageing in both (A4) gut and (B4) brain, independently of the phenotype, when considering either the genes within STEM or the genes within ALL DEGs.

Fig 4. Determining at which age *tert*$^{-/-}$ share more genes associated with the hallmarks of ageing, with the naturally aged WT. (A) Venn diagrams highlight the number of genes associated with hallmarks of ageing in common between old WT (35 months) and *tert*$^{-/-}$ at the different ages tested, in (A.1) gut and (A.2) brain tissues. Data show that the *tert*$^{-/-}$ gut at 2 months has the most number genes associated with hallmarks of ageing in common with old WT gut. The *tert*$^{-/-}$ brain at 22 months has the most number genes associated with hallmarks of ageing in common with old WT brain. The respective lists of genes shared between old WT gut and *tert*$^{-/-}$ gut at 2 months and old WT brain and *tert*$^{-/-}$ 22-month brain is shown in B (B.1 gut, B.2, brain). (B1.1, B1.2) Gene networks with the genes identified in B.1 and B.2 were performed (B1.1 and B1.2, respectively) by K-means clustering using String

software. These include the genes identified in the temporal profiles (from STEM) and in ALL DEGs.

Fig 5. Identifying tert-dependent gene changes in zebrafish gut and brain ageing and their chromosome location in relation to the telomeric end. (A-B) Gene alterations that are anticipated in the *tert*$^{-/-}$ when comparing with WT at the same age (i.e., telomerase-dependent). (A1, B1) Protein-protein interaction network of these genes highlights clusters of genes associated with (A1) metabolic processes in the gut and clusters of genes associated with (B1) cell cycle, genome instability and immune system in the brain. (C)Genes located at the end of the chromosome (i.e., <10MB from chromosome end) are likely to be directly affected by telomere shortening due to the telomere positioning effect (TPE). The data show that there is no significant difference between telomerase-dependent and -independent genes, in what concerns their proximity to the chromosome end, in either gut (C2) or brain (C3). However, there is a significantly higher number of telomerase-dependent genes located at the end of chromosomes in the gut than in the brain (C4).

Fig 6. Determining genes and pathways altered with ageing that are in common between gut and brain. (A) Graph represents WT zebrafish lifespan and highlights 'early' and 'late' stages of ageing. (A.1) All genes identified in common between gut and brain at early (9 months) and late (35 months) stages of ageing. *G and *B represent telomerase-dependent genes in the Gut or in the Brain, respectively. (B-C) Protein-protein interaction networks with the genes found in common between the gut and brain at (B) early and (C) late stages of ageing were performed using STRING software. These include the genes identified in the temporal profiles (from STEM) and in ALL DEGs.

SUPPLEMENTARY FIGURE LEGENDS

Supplementary Fig 1. Genes associated with the hallmarks of ageing that are in common between 35-months-old WT and *tert*$^{-/-}$ at different ages, in the (A1) gut and (A2) brain. The different colours represent different hallmarks of ageing: purple, loss of proteostasis; yellow, mitochondrial dysfunction; green, altered intercellular communication. These include the genes identified in the temporal profiles (from STEM) and in ALL DEGs.

Supplementary Fig 2. Protein-protein interaction network and cluster analysis of gene changes in WT at the 'origins' versus 'later' stages of ageing. (A) Genes identified in common between gut and brain at 9 and 35 months of age. B) Genes significantly altered at "early" and "late" stages of ageing in the gut (B1, 2) and brain (C1, 2), respectively. Network analysis was performed in STRING software and included the genes identified in the temporal profiles (from STEM) and in ALL DEGs. Red squares highlight the protein-protein interaction network of the gene changes that are accelerated in the *tert*$^{-/-}$ (tert-dependent).

1148

1149

1150

1151

Graphical Abstract

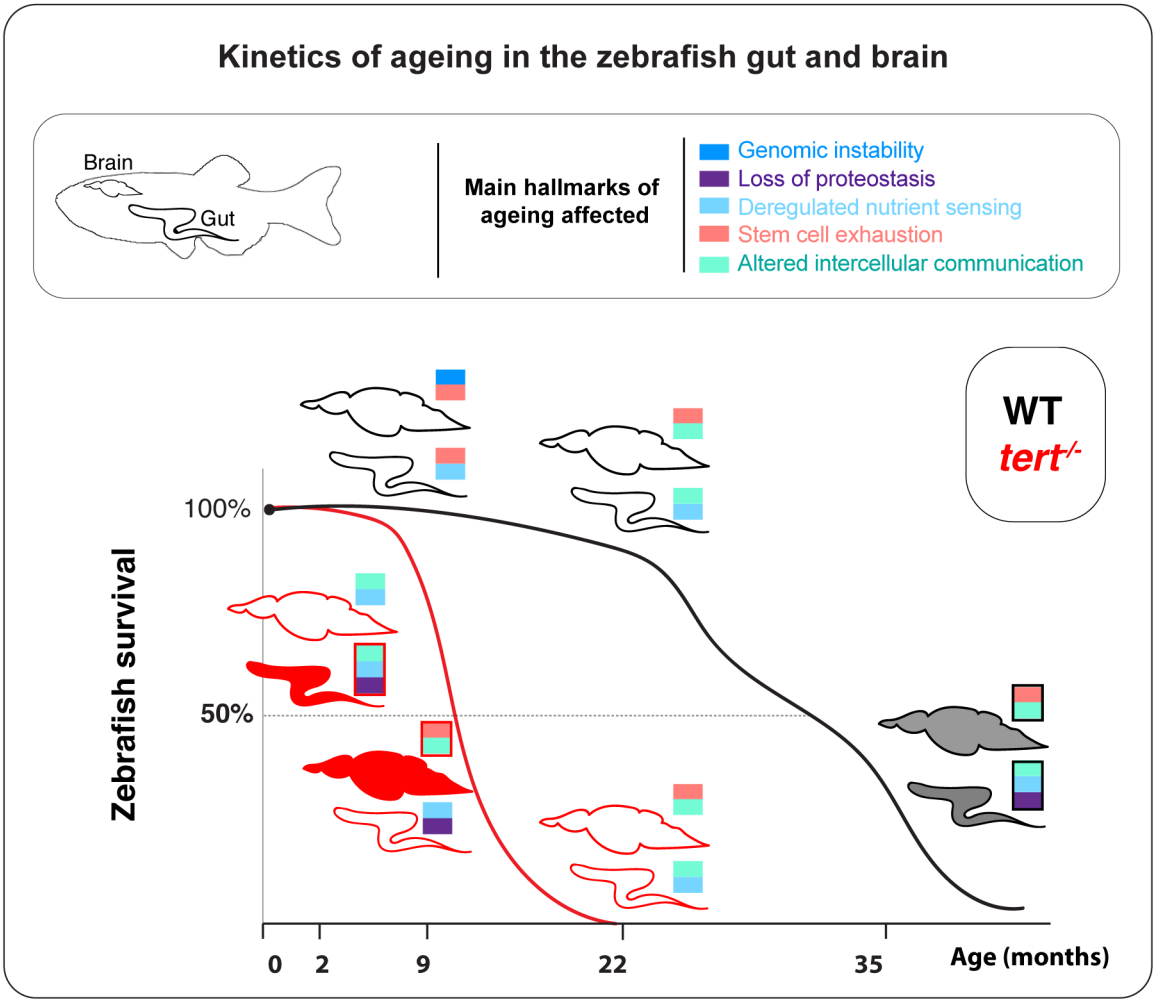

FIGURE 1

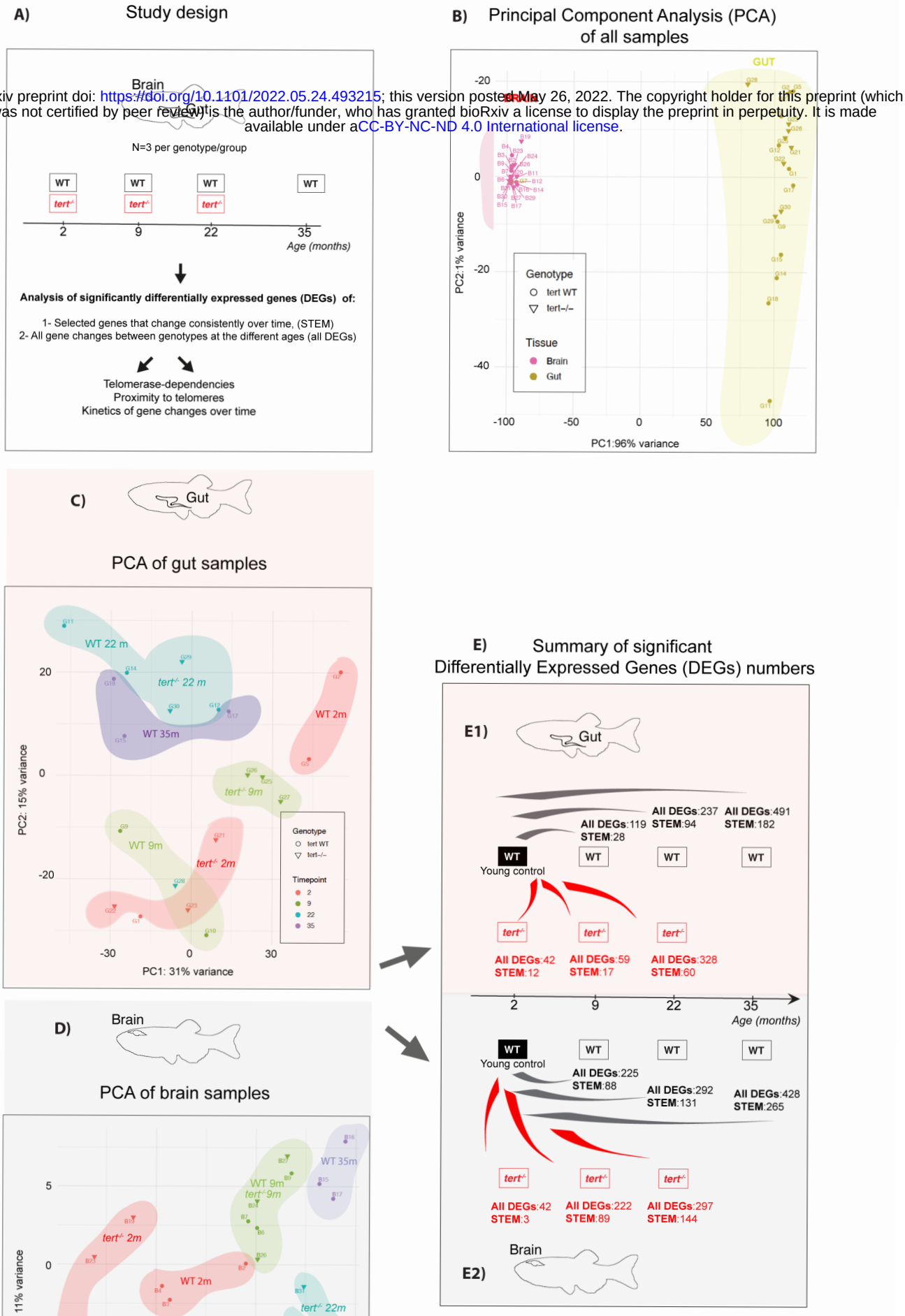

Figure 2 **Signficant STEM profiles and main processes associated, categorised according to known hallmarks of ageing**

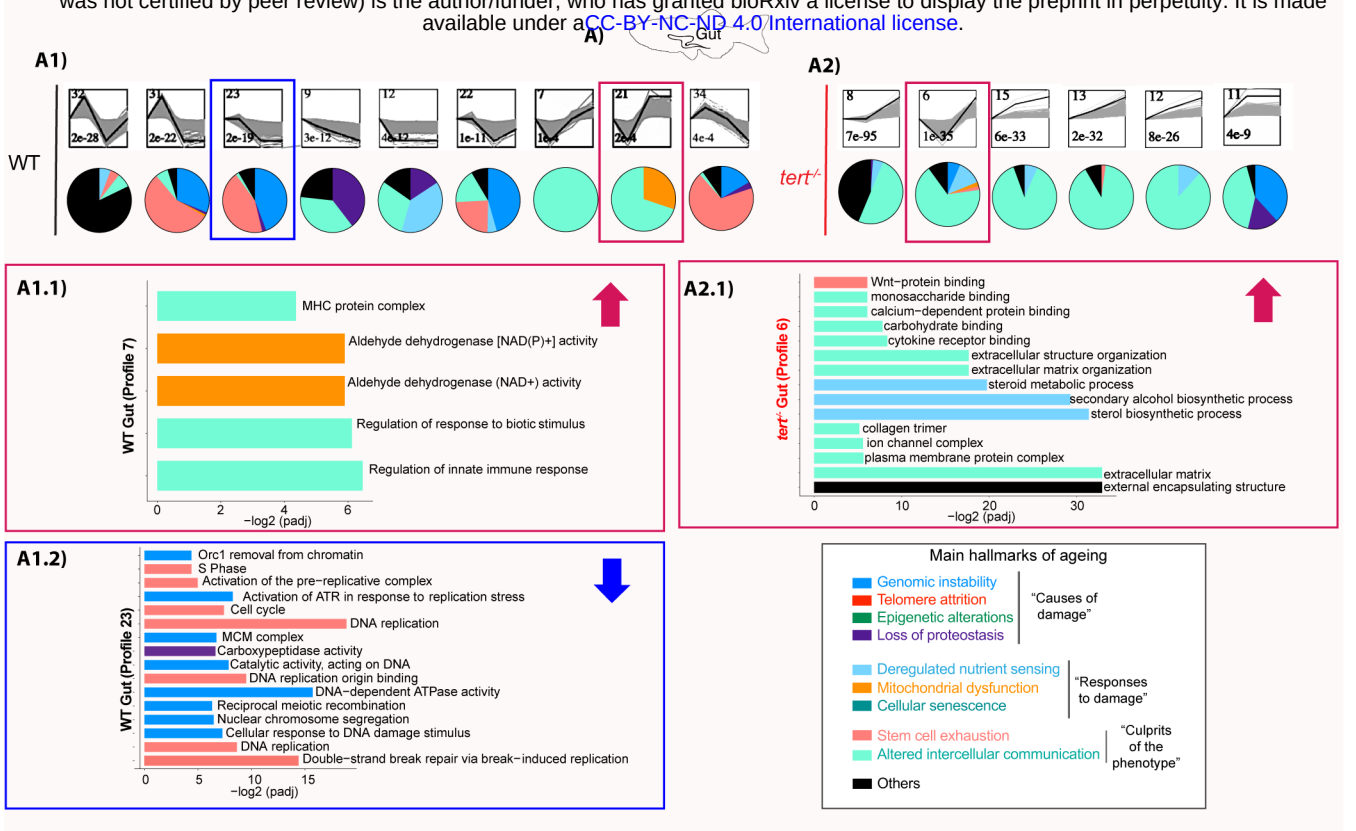

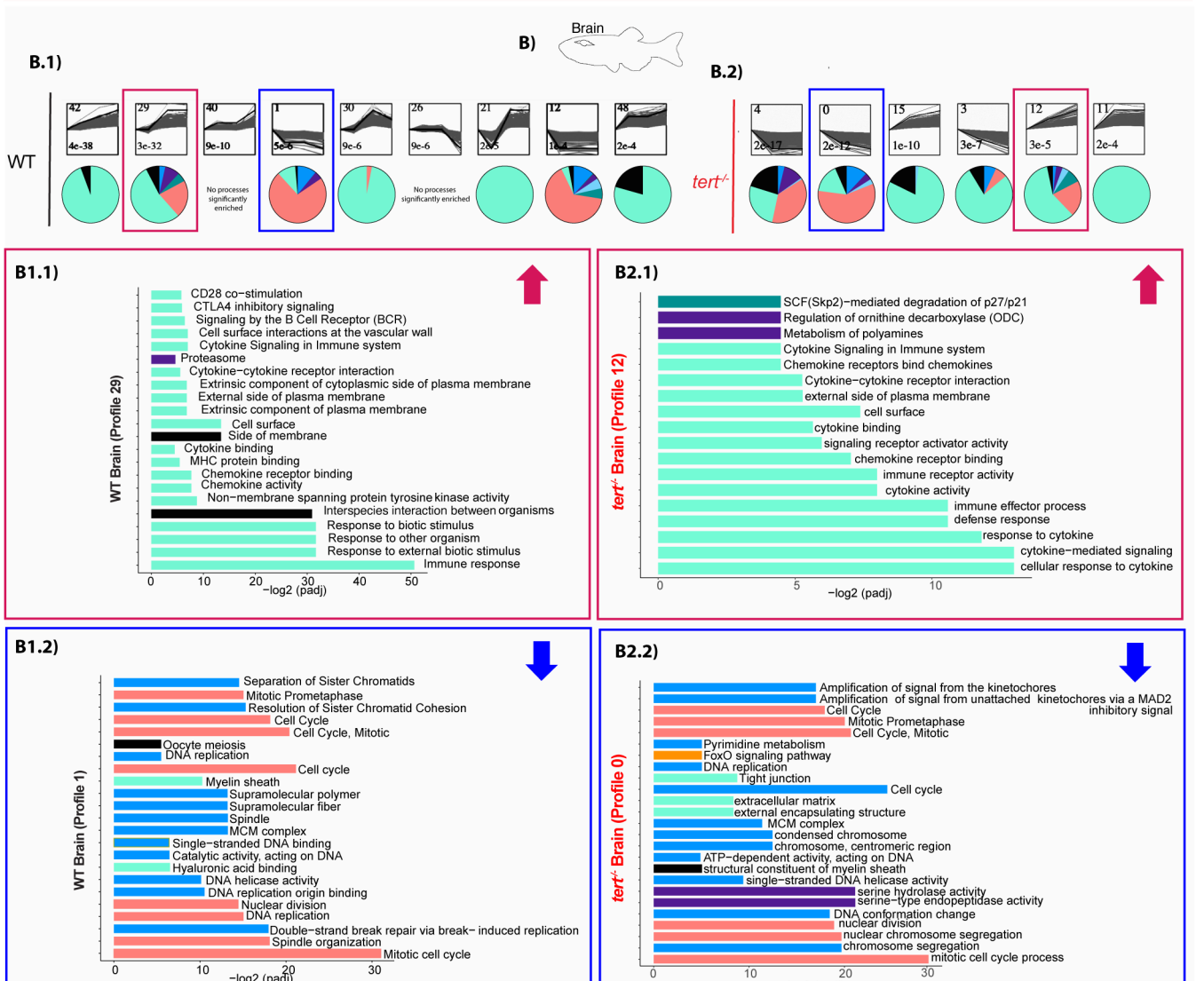

Figure 3 Kinetics of ageing in the zebrafish gut and brain

Main hallmarks of ageing affected

- Genomic instability
- Telomere attrition
- Epigenetic alterations
- Loss of proteostasis
- Deregulated nutrient sensing
- Mitochondrial dysfunction
- Cellular senescence
- Stem cell exhaustion
- Altered intercellular communication
- Others

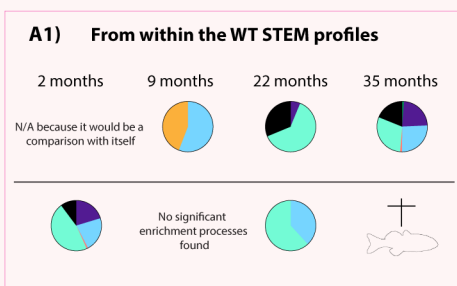

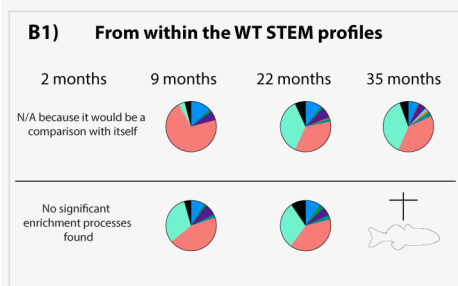

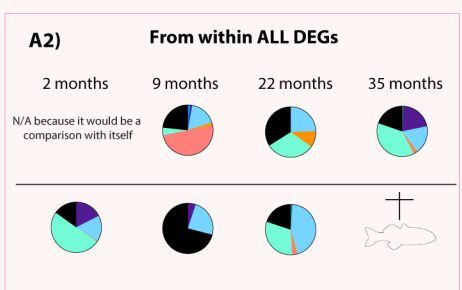

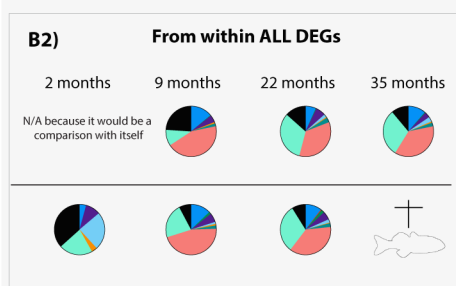

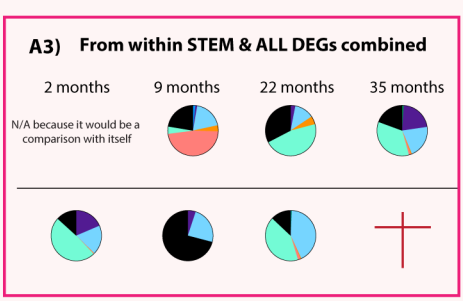

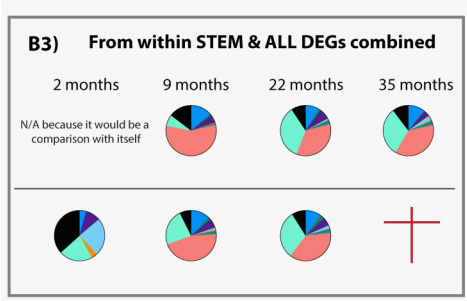

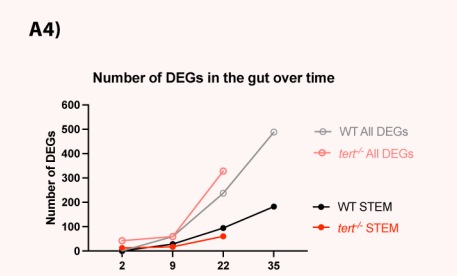

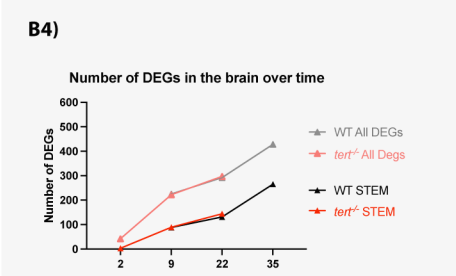

Figure 4

A) Genes associated with the hallmarks of ageing in common between *tert*$^{-/-}$ at the different ages and the aged WT at 35 months

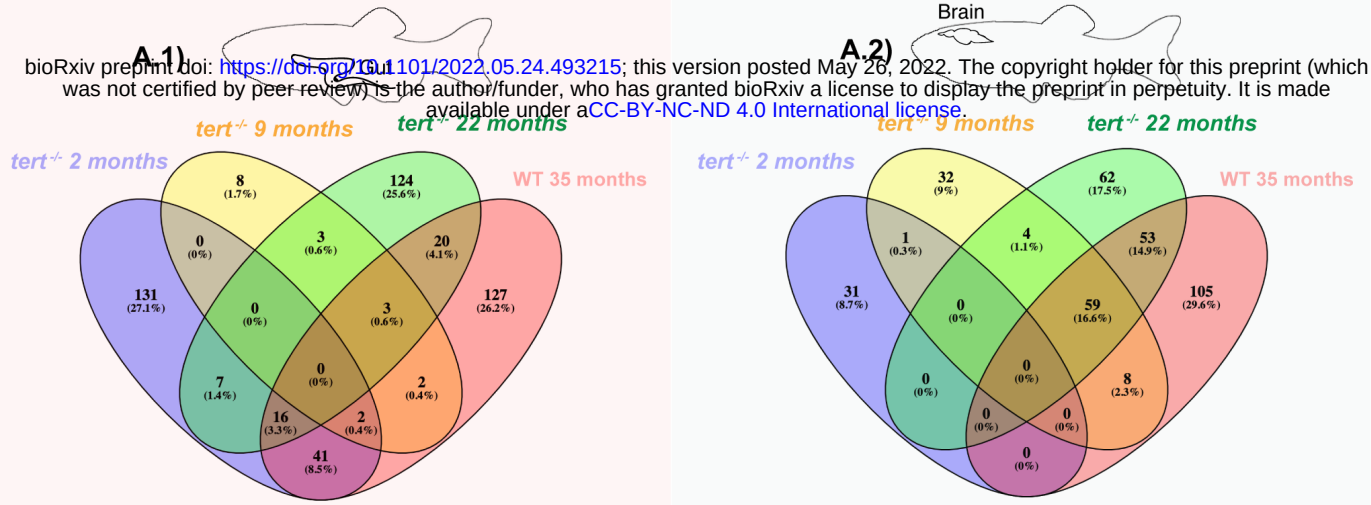

B) Most gene changes shared between *tert*$^{-/-}$ and 35 month old WT, related to the main hallmarks of ageing affected

B.1) GUT

Altered intercellular communication
Deregulated nutrient sensing
Loss of proteostasis

Altered intercellular communication	Deregulated nutrient sensing	Loss of proteostasis
angptl2b	acat1	ahsg1
apoa1b	ces2a	ambp
c8a	ces3	bmp1a
c8b	comtb	c1r
c9	dpys	c3a.6
cyp8b1	fah	c3b.1
lcn15	hao1	c3b.2
pglyrp2	igf2a	f2
slc22a2	igfbp2a	f7
slc27a1b	lipca	f7i
slc38a3a	pla1a	fn1b
slc38a4		furinb
slc7a2		habp2
slco1d1		hpn
tdo2a		mst1
tfa		oxct1b
ttr		prozb
ttyh3b		qsox1
vtnb		sb:cb37
zgc:153031		serpinf2b
zgc:174260		serping1
		si:ch211-262h13.5
		si:ch211-284e20.8

B.2) BRAIN

Stem cell exhaustion
Altered intercellular communication

Stem cell exhaustion			Altered intercellular communication
aspm	insm1a	kif11	acaa1
aurkb	mcm4	kif14	anln
birc5a	mcm5	kif20a	b2m
ccna2	mcm6	kif2c	batf
ccnb1	ncapg	kif4	ccl38.6
ccnjl	ncapg2	kifc1	cd40
cdc20	ncaph	lgals9l1	cd74a
cdk2	nusap1	mad2l1	ch25h
cdk6	prc1b	mcm2	csf1b
cenpe	primpol	ncapd3	cxcl18b
chaf1a	rad54l	ndc80	grem2b
chek1	rrm2	tuba8l3	h3f3b.1
ckap2l	sgo1		h3f3c
dla	si:ch211-244o22.2		hbba2
dlb	smc4		il2rb
dld	spc24		irf8
ercc6l	tacc3		lifrb
fosab	top2a		mhc2a
gadd45gb.1	tpx2		psmb8a
h2af1al	ttk		psme2
hapln1a	tubb5		pyyb
hmmr	uhrf1		rac2
	wdhd1		racgap1
			si:busm1-266f07.2
			spi1a
			stat4
			tlr2
			wasb

B1.1) String Network analysis (K means clustering) GUT

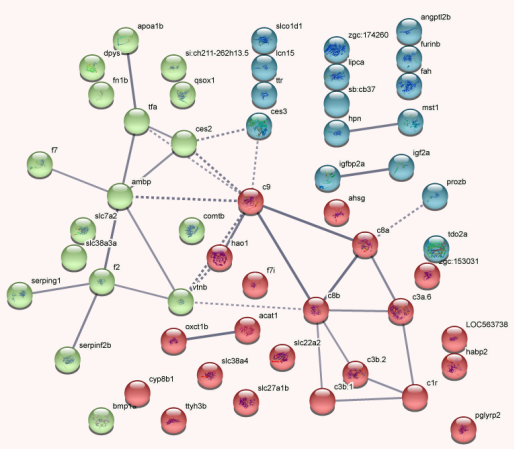

B.2.1) String Network analysis (K means clustering) BRAIN

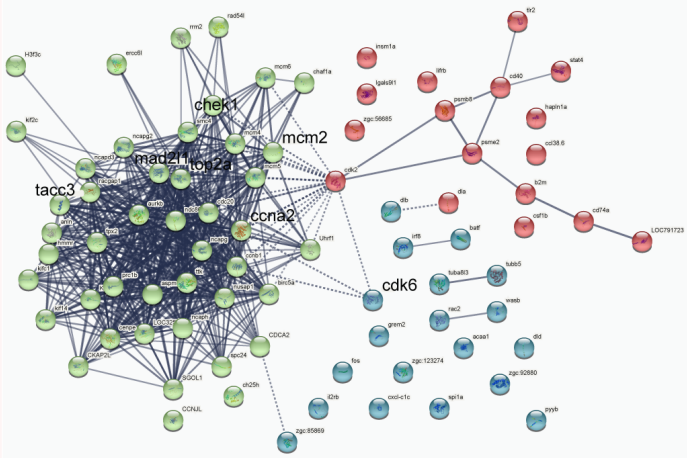

Figure 5

tert-dependent gene changes of old age

A) 

cyp2aa4
ggt5a
kank1b
nrg1
raver1
sytl1
tlr18

acat1
aqp8l
aif1l
angptl3
asgrl1
cfhl2
chia.6
comtb
csad
cyp8b1
f7
fut9
gcat
glceb
hbba1
hmga2
hpn
hsp90b1
igfbp2a
map4k2
me1
mpc2
mpdu1a
nr0b1
oaz2a
osr2
ppfibp1a
prox1a
sephs1
si:ch211-262h13.5
slc1a4
slc22a15
slc22a23
slc27a1b
slc38a3a
slc38a4
sox6
tmed5
ugt5c2
vav3b
zgc:112492

A1)

Protein-protein interaction (PPI) network and cluster analysis

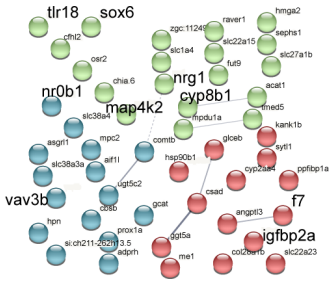

Organic acid metabolic process
Oxoacid metabolic process
Carboxylic acid metabolic process
Metabolic pathways
Monocarboxylic acid metabolic process
Taurine and hypotaurine metabolism
PPAR signaling pathway

C) Chromosome location of *tert*-dependent versus independent gene changes in the gut and brain

C1)

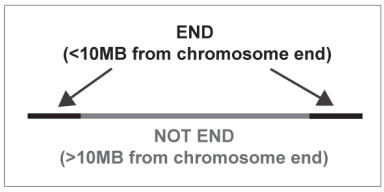

C2)

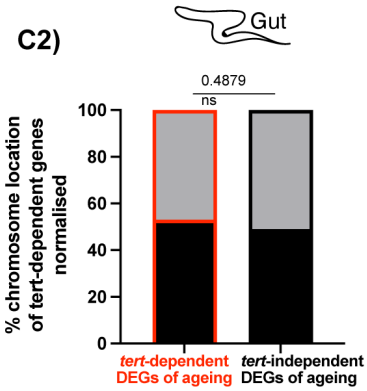

B) 

ankrd22
arfgap3
blf
c1ql3b
calcoco2
cishb
cpeb1b
cry-dash
csf1b
cxcl18b
cyp24a1
ddx43
dicp3.1
dre-mir-29b-1
efemp2b
eif4ebp3l
fbxo32
fcer1gl
fgl2a
fstl3
fthl28
ftr43
fut9
hsd11b2
irf8
lgals9l1
lifrb
mb
mhc2a
pfkfb3
pih1d2
pyyb
slc25a21
socs1a
spi1a
stat4
stm
zc3h7ba
zgc:112148
zgc:153151
zgc:172090

ankrd16
arhgap11a
asf1ba
aurkb
b3gnt7l
birc5a
ccnb1
ccnjl
cdca7a
cdk2
chaf1a
chaf1b
chek1
ckap2l
dbx1a
dld
f10
fabp11a
fosab
h2af1al
h3f3c
helt
hmmr
hsp90aa1.1
iqgap3
kif11
kif14
kif20a
loxl2b
mad2l1
mcm5
mybl2b
ncapd3
ncapg2
ncaph
ndc80
neurod4
nog1
primpol
prss59.1
pvalb1
rad54l
sgo1
si:ch211-244o22.2
si:ch211-69g19.2
sinhcafl
smarcb1b
smc4
sox4a
spc24
spc25
tk1
tpx2
tuba8l3
tyms
uhrf1
unga
zwi

B1)

Protein-protein interaction (PPI) network and cluster analysis

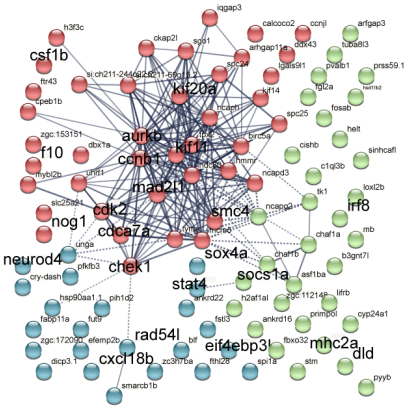

Cell cycle
genome stability
Immune system

C3)

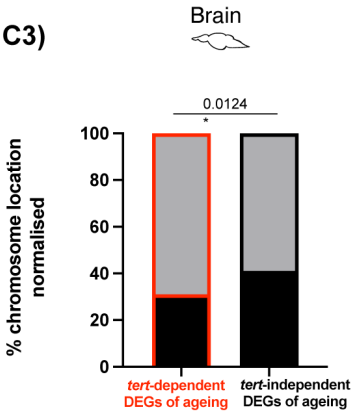

C4)

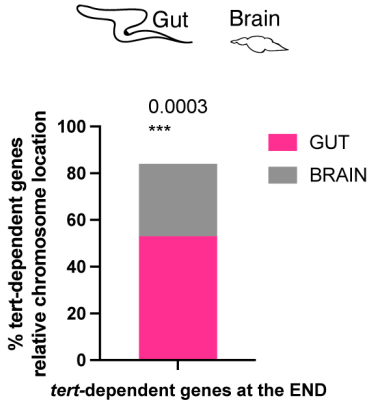

FIGURE 6

Protein-protein interaction (PPI) network and cluster analysis of changes in WT ageing (STEM and All DEGs combined)

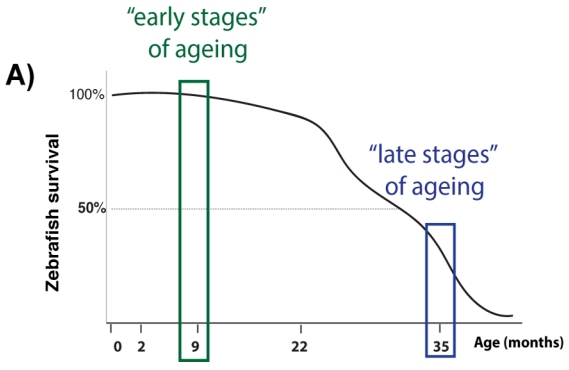

A.1) DEGs shared between gut and brain

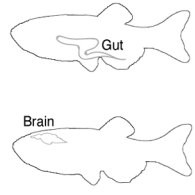

9 months old	35 months old	
*ccnb1 (*B)*	*apoa1b*	*ftr43 (*B)*
cfap45	*b2m*	*gatm*
*eif4ebp3l (*B)*	*cbx7a*	*gbp3*
kif2c	*ccl38.6*	*ggact.2*
serpinh1a	*ccl38a.4*	*ggact.3*
si:ch211-5k11.8	*ccnjl (*B)*	*il2rb*
tmem37	*cd59*	*osr2 (*G)*
	cd99l2	*si:ch211-284e20.8*
	comta	*si:ch211-79k12.1*
	dnmt3ba	*taco1*
	*eif4ebp3l (*B)*	*vav3 (*G)*
	*fabp11a (*B)*	

B) PPI of DEGs shared between gut and brain at 9 months

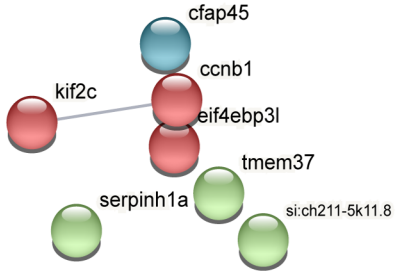

C) PPI of DEGs shared between gut and brain at 35 months

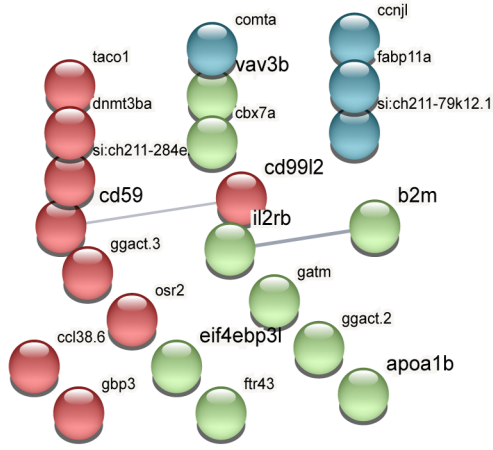

Supp Fig 1

A) **Genes associated with the hallmarks of ageing in common between *tert*$^{-/-}$ at the different ages and the aged WT at 35 months**

A1)

WT 35 months x

tert $^{-/-}$ 2 months		*tert* $^{-/-}$ 9 months	*tert* $^{-/-}$ 22 months
acat1	*sb:cb37*	*acsf2*	***acat1***
ahsg1	*serpinf2b*	***cyp8b1***	*angptl3*
ambp	*serping1*	*hbaa2*	*comtb*
angptl2b	***si:ch211-262h13.5***	*mgll*	*f10*
apoa1b	***si:ch211-284e20.8***	*p4ha2*	***f7***
bmp1a	*slc22a2*	*pla1a*	*fam83d*
c1r	***slc27a1b***	*sephs1*	*gatm*
c3a.6	***slc38a3a***		*gbp3*
c3b.1	***slc38a4***		*gcat*
c3b.2	***slc7a2***		*ggt5a*
c8a	***slco1d1***		*glyctk*
c8b	*tdo2a*		*gpt*
c9	*tfa*		***hpn***
ces2a	***ttr***		*itln2*
ces3	***ttyh3b***		*me1*
comtb	*vtnb*		*mlsl*
cyp8b1	*zgc:153031*		*mpc1*
dpys	*zgc:174260*		***nr0b1***
f2			*nrg1*
f7			*oaz2a*
f7i			*pcbd1*
fah			*pcxa*
fn1b			*pfkfb*
furinb			***prox1a***
habp2			***si:ch211-262h13.5***
hao1			***si:ch211-284e20.8***
hbba1			*slc16a6a*
hpn			*slc1a4*
igf2a			***slc27a1b***
igfbp2a			***slc38a3a***
lcn15			***slc38a4***
lipca			*slc43a1b*
mst1			***slc7a2***
nr0b1			***slco1d1***
oxct1b			***ttr***
pglyrp2			***ttyh3b***
pla1a			*urahb*
prox1a			*vkorc1*
prozb			*zgc:92040*
qsox1			

A2)

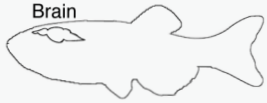

WT 35 months x

tert $^{-/-}$ 9 months		*tert* $^{-/-}$ 22 months		
anln	***mcm6***	*acaa1*	*h3f3b.1*	***plp1b***
arhgap11a	***mybl2b***	***anln***	*h3f3c*	*ppp1r14ba*
aspm	***ncapd3***	*asf1ba*	***hapln1a***	*prc1b*
aurkb	***ncapg***	***aspm***	*hbaa2*	*prdm8*
ccna2	***ncapg2***	***aurkb***	*hbba2*	***primpol***
ccnb1	***ncaph***	*b2m*	*hmmr*	*psmb8a*
cd40	***ndc80***	*batf*	***igf2bp1***	*psme2*
cdc20	***neurod4***	*birc5a*	*il2rb*	*pyyb*
cdk2	***nusap1***	*ccl38.6*	*inab*	*rac2*
cdk6	*orc3*	***ccna2***	***insm1a***	*racgap1*
cenpe	***plp1b***	***ccnb1***	*irf8*	*rad54l*
chaf1b	***primpol***	*ccnjl*	***kif11***	***rrm2***
cyp24a1	***rrm2***	***cd40***	***kif14***	***sgo1***
dbx1a	***sgo1***	*cd74a*	***kif20a***	*si:busm1-266f07.2*
dld	***si:ch211-244o22.2***	***cdc20***	***kif2c***	***si:ch211-244o22.2***
dnmt3aa	***smc4***	***cdk2***	***kif4***	*smarcb1b*
dnmt3ba	*socs1a*	***cdk6***	***kifc1***	***smc4***
ercc6l	***sox4a***	***cenpe***	***lgals9l1***	*sox11a*
f10	***sox4b***	*ch25h*	***lifrb***	***sox4a***
gadd45gb.1	***spc24***	*chaf1a*	***mad2l1***	***sox4b***
hapln1a	*spc25*	*chaf1b*	***marcksa***	***spc24***
hsp90aa1.1	***spi1a***	*chek1*	***mbpb***	***spi1a***
igf2bp1	***tacc3***	*ckap2l*	***mcm2***	*spinb*
insm1a	***top2a***	*csf1b*	*mcm4*	*stat4*
kif11	***tpx2***	*cxcl18b*	***mcm5***	***tacc3***
kif14	***ttk***	*dbx1a*	***mcm6***	*tap2a*
kif20a	***tubb5***	*dla*	*mhc2a*	*tlr2*
kif2c	***tyms***	*dlb*	***mybl2b***	***top2a***
kif4	***uhrf1***	*dld*	***ncapd3***	***tpx2***
kifc1	*unga*	***dnmt3aa***	***ncapg***	***ttk***
lgals9l1		***dnmt3ba***	***ncapg2***	*tuba8l3*
lifrb		***ercc6l***	***ncaph***	***tubb5***
mad2l1		*fosab*	***ndc80***	***tyms***
marcksa		*foxn4*	*nefmb*	*ube2c*
mbpb		***gadd45gb.1***	***neurod4***	*uhrf1*
mcm2		*grem2b*	***nusap1***	*wasb*
mcm5		*h2af1al*	*plp1a*	*wdhd1*
				zwi

Supp Fig 2
Protein-protein interaction network and cluster analysis of changes in WT ageing (STEM and All DEGs combined)